3.1 CYLINDERS.

A better understanding of the theory of buckling of circular cylindrical shells has been made possible by use of electronic digital computers. This understanding has been aided both by more rigorous formulations of the theory and by reliance on experimental investigation.

Most of the available information on buckling of circular cylindrical shells is restricted to unstiffened shells of uniform thickness or to stiffened shells with uniform stiffness and properties, subjected to axisymmetric loading states which have certain simple longitudinal distributions, generally uniform. Problems involving surface loadings and thickness or stiffness variations that are axisymmetric but nonuniform longitudinally have been solved, but detailed investigations of the effects of various parameters have not been made. Also, available information is inadequate for the analysis of loadings that are nonuniform circumferentially. Problems of this type can be treated by digital computer programs and will be discussed in Subsection 3.4.

The application of theory to the design of actual cylindrical shells has been complicated by apparent discrepancies between theory and experiment. For shells in which longitudinal compression of the cylinder wall predominates, the discrepancies can be quite large. For shells in which shear or circumferential compression predominates, the discrepancies are generally less severe but still large enough to require experimental programs to establish design data. The causes of such discrepancies are generally understood.

The primary source of error is the dependence of the buckling load of cylindrical shells on small deviations from the nominal circular cylindrical shape of the structure. Because the unloaded shape of a test specimen usually has not been stringently controlled, most test results for

nominally identical specimens have larger scatter and fall below the theoretical values.

Another source of discrepancy is the dependence of buckling loads of cylindrical shells on edge values of longitudinal and circumferential displacements or forces. Also, because tangential edge conditions have not usually been precisely controlled in buckling tests, some of the scatter of test results can be attributed to this source. Current methods of establishing design data tend to treat both initial imperfections and edge conditions as random effects. Results from all available tests are considered together without regard to specimen construction or methods of testing and are analyzed to yield lower bound or statistical correction factors to be applied to simplified versions of the theoretical results. This technique has proved satisfactory to date for design purposes.

Within the limitations imposed by the state of the art, acceptable procedures for the estimation of critical loads on circular cylindrical shells are described in this section.

3.1.1 ISOTROPIC UNSTIFFENED CYLINDERS.

Unstiffened isotropic circular cylinders subjected to various conditions of loading are considered below.

3.1.1.1 Axial Compression — Unpressurized.

The design allowable buckling stress for a circular cylinder subjected to axial compression is given by

$$\frac{\sigma_{x_{cr}}}{\eta} = \frac{\gamma E\, t/r}{\sqrt{3\,(1-\mu^2)}} \qquad (1)$$

$$\frac{\sigma_{x_{cr}}}{\eta} = 0.6\,\gamma\,\frac{Et}{r} \quad (\text{for } \mu = 0.3) \quad ,$$

where the factor γ should be taken as

$$\gamma = 1.0 - 0.901\ (1-e^{-\phi}) \qquad (2)$$

where

$$\phi = \frac{1}{16}\sqrt{\frac{r}{t}} \quad \text{for} \quad (\frac{r}{t} < 1500)$$

Equation (2) is shown graphically in Figure 3.1-1 and provides a good lower bound for most test data [6]. The information in Figure 3.1-1 should be used with caution for cylinders with length-radius ratios greater than about five since the correlation has not been verified by experiment in this range. Very long cylinders should be checked for Euler-column buckling.

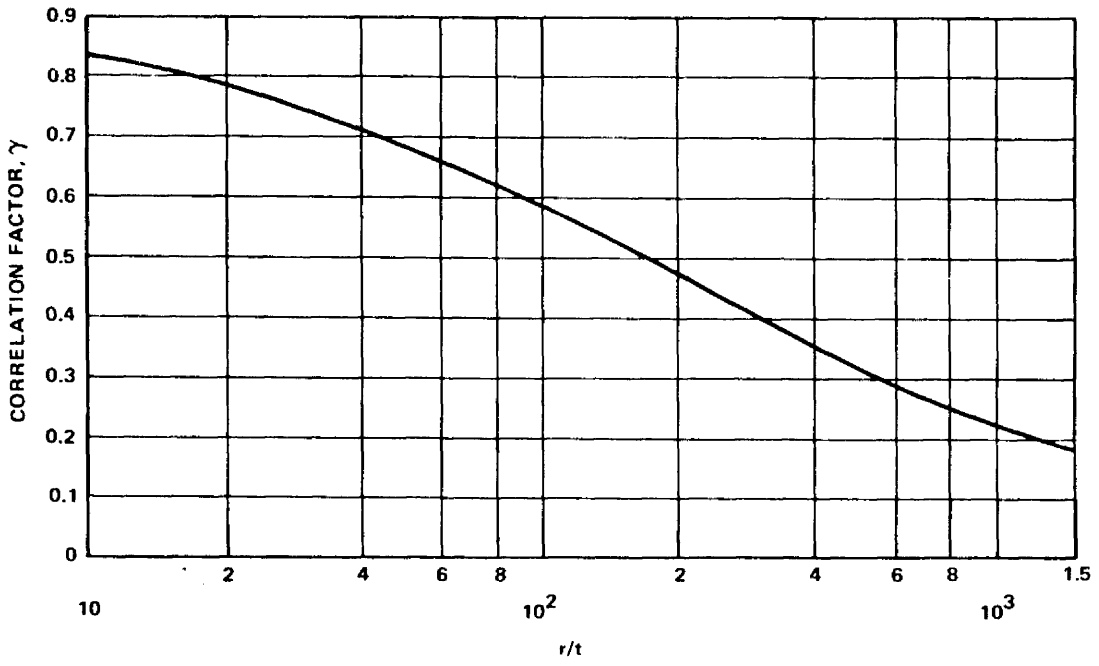

FIGURE 3.1-1. CORRELATION FACTORS FOR ISOTROPIC CIRCULAR CYLINDERS SUBJECTED TO AXIAL COMPRESSION

When geometric and material properties are such that the computed buckling stress $\frac{\sigma_{x_{cr}}}{\eta}$ is in the plastic range, the actual buckling stress $\sigma_{x_{cr}}$ should be calculated by applying the plasticity coefficient, η. This calculation is facilitated by the use of the curves of Paragraph 3.1.6. For moderately long cylinders the critical stress $\sigma_{x_{cr}}$ should be determined by using curve E_1 in Paragraph 3.1.6. For extremely short cylinders ($Z \rightarrow 0$) curve G should be used.

For a cylinder having a length between those lengths for which curves E_1 and G apply, a plasticity factor is not available. Presumably, a linear interpolation should provide satisfactory results. Such a factor would be a function of cylinder geometry as well as of the usual material stress-strain curve.

3.1.1.2 Axial Compression — Pressurized

Buckling and collapse coincide for internally pressurized circular cylinders in axial compression, just as in the case of the unpressurized cylinder. Pressurization increases the buckling load in the following ways:

1. The total compressive load must be greater than the tensile pressurization load $p \pi r^2$ before buckling can occur.

2. The destabilizing effect of initial imperfections is reduced. The circumferential tensile stress induced by the pressurization inhibits the diamond buckling pattern, and, at sufficiently high pressurization, the cylinder buckles in the classical axisymmetric mode at approximately the classical buckling stress.

It is recommended that the total load for buckling, unless substantiated by testing, be obtained by the addition of the pressurization load $p \pi r^2$, the buckling load for the unpressurized cylinder [equation (1)], and an increase in the buckling load caused by pressurization; that is:

$$P_{press} = 2 \pi Et^2 \left(\frac{\gamma}{\sqrt{3\,(1-\mu^2)}} + \Delta\gamma \right) + p \pi r^2 \qquad (3)$$

where $\Delta\gamma$ is obtained from Figure 3.1-2.

For $\mu = 0.3$,

$$P_{press} = 2 \pi Et^2 \,(0.6\gamma + \Delta\gamma) + p \pi r^2 \quad . \qquad (4)$$

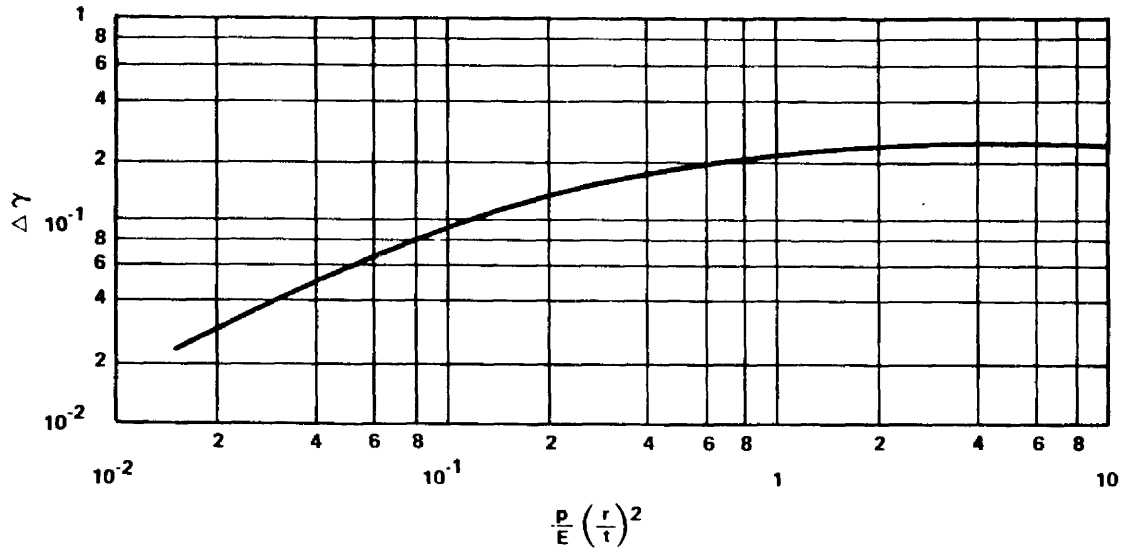

FIGURE 3.1-2. INCREASE IN AXIAL-COMPRESSIVE BUCKLING-STRESS COEFFICIENT OF CYLINDERS RESULTING FROM INTERNAL PRESSURE

3.1.1.3 Bending — Unpressurized.

Buckling and collapse coincide for isotropic, unpressurized circular cylinders in bending. The procedure given for isotropic cylinders in axial compression may be used also to obtain the critical maximum stress for isotropic cylinders in bending, except that a correlation factor based on bending tests should be used in place of the factor given by equation (2) for cylinders in axial compression. The correlation factor for the cylinder in bending is taken as

$$\gamma = 1.0 - 0.731\ (1-e^{-\phi}) \qquad (5)$$

where

$$\phi = \frac{1}{16}\sqrt{\frac{r}{t}}$$

Equation (5) is presented graphically in Figure 3.1-3. This equation should be used with caution for $r/t > 1500$ because experimental data are not available in this range [7]. Although the theoretical critical stress for axial compression and that for bending are the same, the correlation factor for bending is greater than that for compression. This is primarily because the buckling of a cylinder in compression can be triggered by any imperfection on the shell surface, whereas in bending, buckling is generally initiated in the region of the greatest compressive stress.

For inelastic buckling the critical stress may be found by using curves E_t in Paragraph 3.1.6. If the stresses are elastic the allowable moment is

$$M_{cr} = \pi r^2 \sigma_{x_{cr}} t \qquad (6)$$

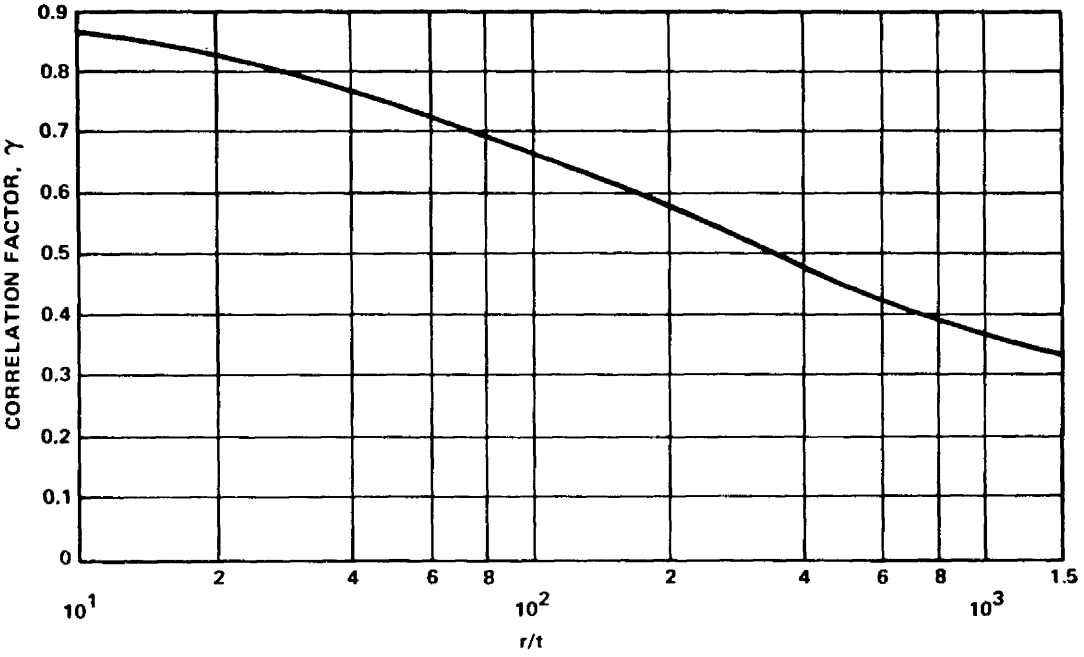

FIGURE 3.1-3. CORRELATION FACTORS FOR ISOTROPIC CIRCULAR CYLINDER SUBJECTED TO BENDING

3.1.1.4 Bending – Pressurized.

For thin-walled cylinders subjected to bending and internal pressure, it is recommended that the buckling moment be obtained by adding the moment-carrying capability of a pressurized membrane cylinder the buckling moment for the unpressurized cylinder [equations (1) and (5)], and an increase in the critical moment caused by pressurization. Then

$$M_{press} = \pi r Et^2 \left(\frac{\gamma}{\sqrt{3\,(1-\mu^2)}} + \Delta\gamma \right) + 0.5\, p\, \pi\, r^3 \quad , \qquad (7)$$

where $\Delta\gamma$ is obtained from Figure 3.1-2.

For $\mu = 0.3$,

$$M_{press} = \pi r Et^2 (0.6\gamma + \Delta\gamma) + 0.5 p \pi r^3 \quad . \quad (8)$$

3.1.1.5 External Pressure.

The term "lateral pressure" designates an external pressure which acts only on the curved walls of the cylinder and not on the ends. The load in the cylinder wall is given by

$$N_y = \sigma_y t = pr \quad . \quad (9)$$

The term "hydrostatic pressure" designates an external pressure which acts on both the curved walls and the ends of the cylinder. The cylinder wall loads are given by

$$N_y = \sigma_y t = pr \quad ,$$

$$N_x = \sigma_x t = \frac{pr}{2} \quad . \quad (10)$$

Except for unusually short cylinders, the critical pressures for the two types of loads are not significantly different.

An approximate buckling equation for supported cylinders loaded by lateral pressure is given as

$$N_{y_{cr}} = k_y \frac{\pi^2 D}{r \ell^2} \quad . \quad (11)$$

The buckling equation for cylinders loaded by hydrostatic pressure is obtained by replacing k_y by k_p in the formula above.

As shown in Figure 3.1-4, except for unusually short cylinders, the critical pressures for the two types of loads are not significantly different. For short cylinders equations suitable for design solutions to the hydrostatic ($Z < 30$) and lateral ($Z < 70$) cases respectively are:

$$k_y = 1.853 + .141714\ Z^{.83666} \tag{12a}$$

and

$$k_y = 3.980 + .02150\ Z^{1.125} \quad . \tag{12b}$$

The solutions for intermediate length cylinders ($100 \leq Z \leq 4000$) converge to an equation given by

$$k_y = .780\sqrt{Z} \tag{13a}$$

or the critical pressure is given by

$$p = \frac{.04125}{(1-\mu^2)^{3/4}} \quad \frac{E}{\left(\frac{r}{t}\right)^{5/2}\left(\frac{\ell}{r}\right)} \quad . \tag{13b}$$

The family of curves for long cylinders ($Z > 3000$) is dependent upon the radius-thickness ratio of the cylinder and corresponds to buckling of the cylinder into an oval shape, as given by

$$k_y = \frac{2.70}{\pi^2} \quad \frac{Z}{\frac{r}{t}\sqrt{1-\mu^2}} \tag{14a}$$

or

$$p = \frac{E}{4(1-\mu^2)} \left(\frac{t}{r}\right)^3 \tag{14b}$$

and applies for $20 \leq \frac{r}{t}\sqrt{1-\mu^2} \leq 100$.

☆U.S. GOVERNMENT PRINTING OFFICE 1976-641-255/391 REGION NO. 4

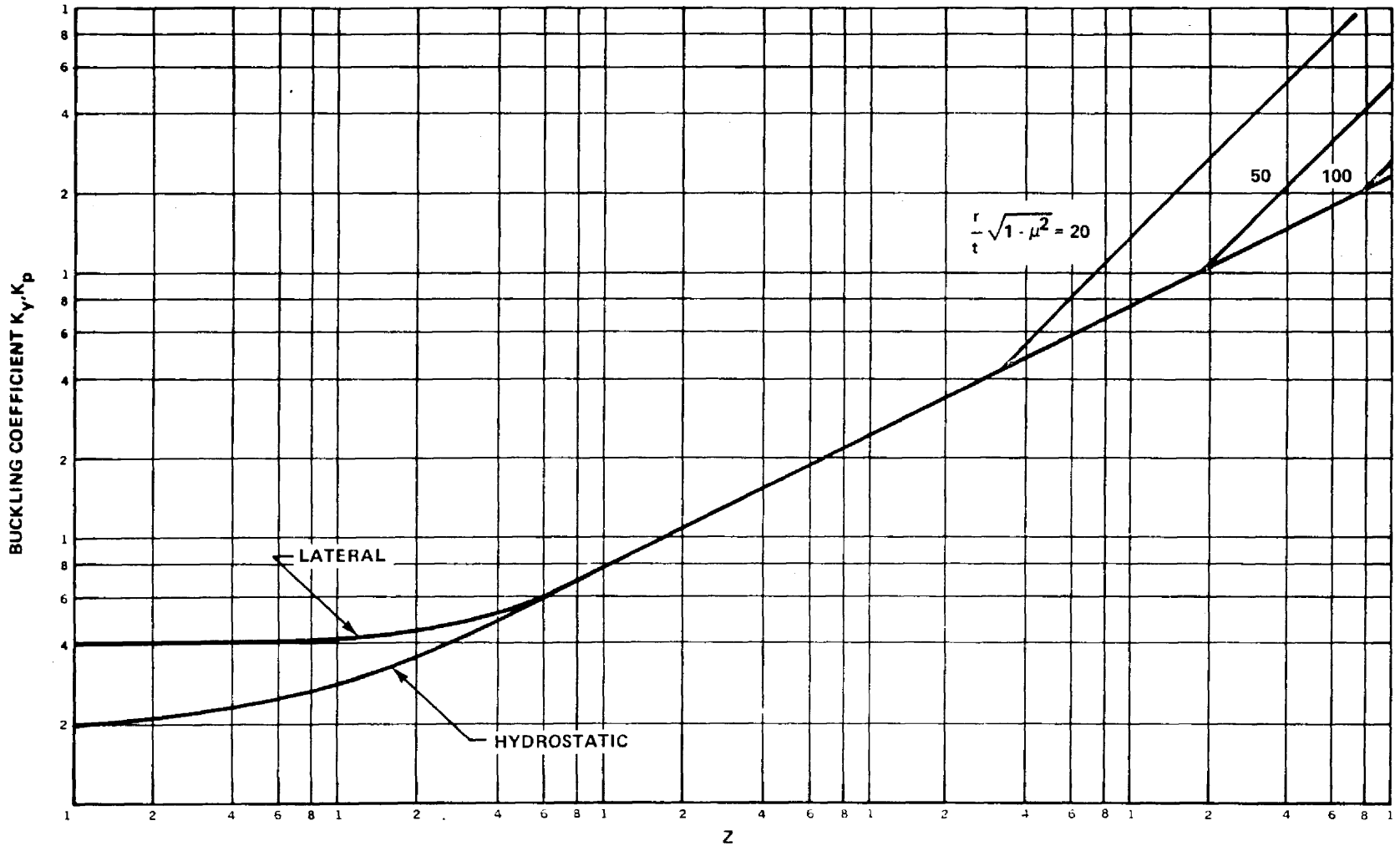

FIGURE 3.1-4. BUCKLING COEFFICIENTS FOR SIMPLY SUPPORTED ISOTROPIC CIRCULAR CYLINDERS SUBJECTED TO EXTERNAL PRESSURE

For inelastic stresses the plasticity correction factor should be obtained from Paragraph 3.1.6. For short cylinders ($\gamma Z < 5$) the C curves should be used. For moderate length cylinders ($5 < \gamma Z < 4000$) the E_1 curve should be used. For long cylinders ($\gamma Z > 4000$) the E curve should be used.

3.1.1.6 Shear or Torsion — Unpressurized.

The theoretical buckling coefficient for cylinders in torsion can be obtained from Figure 3.1-5. The straight-line portion of the curve is given by the equation

$$k_{xy} = \frac{N_{xy}\, \ell^2}{\pi^2 D} = 0.85\ (\gamma Z)^{3/4} \tag{15}$$

and applies for $50 < \gamma Z < 78\ (\frac{r}{t})^2\ (1-\mu^2)$. Equation (15) can be written as

$$\tau_{xy_{cr}} = \frac{0.747\ \gamma^{3/4}\ E}{(\frac{r}{t})^{5/4}\ (\frac{\ell}{r})^{1/2}} \tag{16}$$

For $\gamma Z > 78\ (\frac{r}{t})^2\ (1-\mu^2)$, the cylinder buckles with two circumferential waves. The buckling coefficient is then given by

$$k_{xy} = \frac{2\sqrt{2}\,\gamma Z}{\pi^2\ (\frac{r}{t})^{1/2}\ (1-\mu^2)^{1/4}} \tag{17}$$

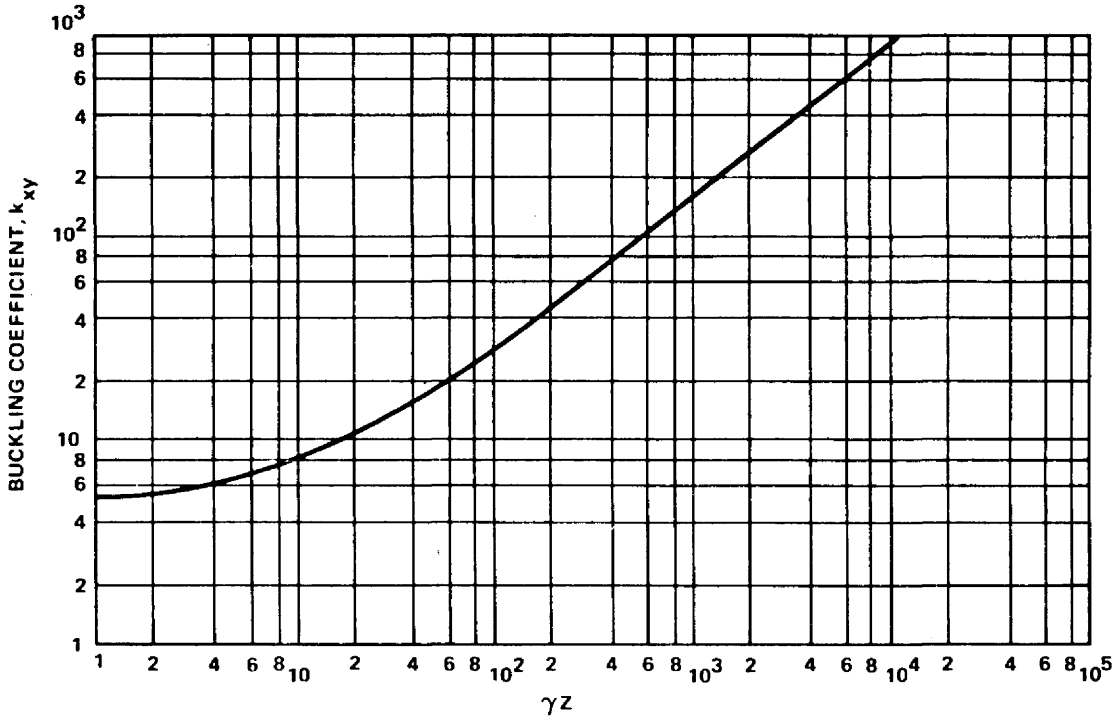

FIGURE 3.1-5. BUCKLING COEFFICIENTS FOR SIMPLY SUPPORTED ISOTROPIC CIRCULAR CYLINDERS SUBJECTED TO TORSION

or

$$\tau_{xy_{cr}} = \frac{\gamma E}{3\sqrt{2}\,(1-\mu^2)^{3/4}} \left(\frac{t}{r}\right)^{3/2} . \qquad (18)$$

To approximate the lower limit of most data, the value

$$\gamma^{3/4} = 0.67 \qquad (19)$$

is recommended for moderately long cylinders.

Plasticity should be accounted for by using curves A in Paragraph 3.1.6.

3.1.1.7 Shear or Torsion — Pressurized.

The increase in buckling stress caused by internal pressure may be calculated by using the curves in Reference 1.

3.1.1.8 Combined Loading.

The criterion for structural failure of a member under combined loading is frequently expressed in terms of a stress-ratio equation, $R_1^x + R_2^y + R_3^z = 1$. The subscripts denote the stress caused by a particular kind of loading (compression, shear, etc.), and the exponents (usually empirical) express the general relationship of the quantities for failure of the member. Simply stated, the term "stress-ratio" is used to denote the ratio of applied to allowable stress.

I. Axial Compression and Bending.

The recommended interaction equation for combined compressive load and bending is

$$R_c + R_b = 1 \quad . \tag{20}$$

The quantities R_c and R_b are, respectively, the compressive and bending load or stress ratios. The denominators of the ratios are the allowable loads or stresses given by equations (1) and (2) for cylinders in axial compression and by equations (1) and (5) for cylinders in bending.

Equation (20) is also recommended for internally pressurized circular cylinders in combined axial compression and bending by using equations (3) or (4) and (7) or (8).

II. Axial Compression and External Pressure.

The recommended interaction equation for combined compressive load and hydrostatic or lateral pressure is

$$R_c + R_p = 1 \quad . \tag{21}$$

The quantities R_c and R_p are, respectively, the compressive and hydrostatic or lateral pressure load or stress ratios. The denominators of the ratios are the allowable stresses given by equations (1) and (2) for cylinders in axial compression and by equations (11) or (12) for cylinders subjected to external pressure.

III. Axial Compression and Torsion.

For cylindrical shells under torsion and axial compression, the analytical interaction curve is a function of Z and varies from a parabolic shape at low-Z values to a straight line at high-Z values. The scatter of experimental data suggests the use of a straight-line interaction formula. Therefore, the recommended interaction equation is

$$R_c + R_t = 1 \quad . \tag{22}$$

The quantities R_c and R_t are, respectively, the compressive and torsion load or stress ratios. The denominators of the ratios are the allowable stresses given by equations (1) and (2) for cylinders in axial compression and by equations (16) or (18) for cylinders in torsion.

IV. Bending and Torsion.

A conservative estimate of the interaction for cylinders under combined bending and torsion is

$$R_b + R_t^2 = 1 \quad . \tag{23}$$

The quantities R_b and R_t are, respectively, the bending and torsion load or stress ratios. The denominators of the ratios are the allowable stresses given by equations (1) and (5) for cylinders in bending and by equations (16) or (18) for cylinders in torsion.

3.1.2 ORTHOTROPIC CYLINDERS.

The term "orthotropic cylinders" covers a wide variety of cylinders. In its strictest sense, it denotes cylinders made of a single orthotropic material or of orthotropic layers. It also denotes types of stiffened cylinders for which the stiffener spacing is small enough for the cylinder to be approximated by a fictitious sheet whose orthotropic bending and extensional properties include those of the individual stiffening elements averaged out over representative widths or areas. Generally, the directions of the axes of orthotropy are taken to coincide with the longitudinal and circumferential directions of the cylinder.

The behavior of the various types of orthotropic cylinders may be described by a single theory, the elements of which are equations of equilibrium for the buckled structure, relationships between force and moment resultants, and extensional and bending strains. For cylinders of a single orthotropic material, it is generally permissible to neglect the coupling between force resultants and bending strains and between moment resultants and extensional strains. The theory is then similar to that for isotropic cylinders.' For stiffened cylinders or for cylinders having orthotropic layers, however, neglect of the coupling terms can lead to serious errors. For example, the inclusion of coupling terms yields a significant difference in theoretical results for stiffened cylinder configurations having stiffeners on the inner surface or the outer surface. The difference vanishes when coupling is omitted.

Theoretical and experimental results for stiffened shells are generally in better agreement than those for unstiffened shells. The possibility of local buckling of the cylinder between stiffening elements should be checked.

In general, the complexity of the analysis for orthotropic cylinders necessitates the use of a computer solution. Applicable computer solutions are discussed in Subsection 3.4.

3.1.2.1 Axial Compression.

A buckling equation for stiffened orthotropic cylinders in compression [8] is given by:

$$N_x = \left(\frac{\ell}{m\pi}\right)^2 \frac{\begin{vmatrix} A_{11} & A_{12} & A_{13} \\ A_{21} & A_{22} & A_{23} \\ A_{31} & A_{32} & A_{33} \end{vmatrix}}{\begin{vmatrix} A_{11} & A_{12} \\ A_{21} & A_{22} \end{vmatrix}} \quad \text{for} \quad (n \geq 4) \quad , \qquad (24)$$

in which

$$A_{11} = \overline{E}_x \left(\frac{m\pi}{\ell}\right)^2 + \overline{G}_{xy}\left(\frac{n}{r}\right)^2 \quad . \qquad (25)$$

$$A_{22} = \overline{E}_y \left(\frac{n}{r}\right)^2 + \overline{G}_{xy}\left(\frac{m\pi}{\ell}\right)^2 \quad . \qquad (26)$$

$$A_{33} = \overline{D}_x \left(\frac{m\pi}{\ell}\right)^4 + \overline{D}_{xy} \left(\frac{m\pi}{\ell}\right)^2 \left(\frac{n}{r}\right)^2 + \overline{D}_y \left(\frac{n}{r}\right)^4$$

$$+ \frac{\overline{E}_y}{r^2} + \frac{2\overline{C}_y}{r} \left(\frac{n}{r}\right)^2 + \frac{2\overline{C}_{xy}}{r} \left(\frac{m\pi}{\ell}\right)^2 \quad . \qquad (27)$$

$$A_{12} = A_{21} = \left(\overline{E}_{xy} + \overline{G}_{xy}\right) \frac{m\pi}{\ell} \frac{n}{r} \quad . \qquad (28)$$

$$A_{23} = A_{32} = \left(\overline{C}_{xy} + 2\overline{K}_{xy}\right) \left(\frac{m\pi}{\ell}\right)^2 \frac{n}{r} + \frac{\overline{E}_y n}{r^2} + \overline{C}_y \left(\frac{n}{r}\right)^3 \quad . \qquad (29)$$

$$A_{31} = A_{13} = \frac{\overline{E}_{xy}}{r} \frac{m\pi}{\ell} + \overline{C}_x \left(\frac{m\pi}{\ell}\right)^3 + \left(\overline{C}_{xy} + 2\overline{K}_{xy}\right) \frac{m\pi}{\ell} \left(\frac{n}{r}\right)^2 \quad . \qquad (30)$$

Values of stiffeners to be used for various types of construction are given in Paragraph 3.1.2.6. Prebuckling deformations are not taken into account in the derivation of the equation. The cylinder edges are assumed to be supported by rings that are rigid in their own plane but offer no resistance to rotation or bending out of their plane. The equation can be specialized for various types of cylinders which have been treated separately in the literature; for example, unstiffened or stiffened orthotropic cylinders with eccentricity effects neglected and stiffened or stiffened orthotropic cylinders with eccentricity effects taken into account. For ring-stiffened corrugated cylinders, a similar but not identical theory is given in References 9 and 10. For given cylinder and stiffener dimensions, the values of m and n to be used are those which minimize $\overline{N}_x$.

The unusually large number of parameters in equation (24) does not permit any definitive numerical results to be shown. The computer programs discussed in Subsection 3.4 should be used for solution of the critical axial compressive load for a given design. It has been shown that for combinations of parameters representative of stiffened shells, calculations indicate that external stiffening, whether stringers or rings or both, can be more effective than internal stiffening for axial compression. Generally, calculations neglecting stiffener eccentricity yield unconservative values of the buckling load for internally stiffened cylinders and conservative values of the buckling load for externally stiffened cylinders. An extensive investigation of the variation of the buckling load with various stiffener parameters is reported in Reference 11. The limited experimental data [9-17] for stiffened shells are in reasonably good agreement with the theoretical results for the range of parameters investigated.

On the basis of available data, it is recommended that the buckling loads [calculated from equation (24)] of cylinders having closely spaced, moderately large stiffeners be multiplied by a factor of 0.75. The correlation coefficients covering the transition from unstiffened cylinders to stiffened cylinders with closely spaced stiffeners have not been fully investigated. Although theory and experiment [16] indicate that restraint against edge rotation and longitudinal movement significantly increases the buckling load, not enough is known about the edge restraint of actual cylinders to warrant taking advantage of these effects unless such effects are substantiated by tests.

For layered or unstiffened orthotropic cylindrical shells, the available test data are quite meager [18, 19]. For configurations where the coupling coefficients $\overline{C}_x$, $\overline{C}_y$, $\overline{C}_{xy}$, and $\overline{K}_{xy}$ can be neglected,

it is recommended that the buckling load be calculated from the equation

$$\frac{N_x \ell^2}{\pi^2 \overline{D}_x} = m^2 \left(1 + 2 \frac{\overline{D}_{xy}}{\overline{D}_x} \beta^2 + \frac{\overline{D}_y}{\overline{D}_x} \beta^4 \right)$$

$$+ \frac{\gamma^2 \ell^4}{\pi^4 m^2 \overline{D}_x r^2} \frac{\overline{E}_x \overline{E}_y - \overline{E}^2_{xy}}{\overline{E}_x + \left(\frac{\overline{E}_x \overline{E}_y - \overline{E}^2_{xy}}{\overline{G}_{xy}} - 2\overline{E}_{xy} \right) \beta^2 + \overline{E}_y \beta^4} . \tag{31}$$

The correlation factor γ is taken to be of the same form as the correlation factor for isotropic cylinders [equation (2)] with the thickness replaced by the geometric mean of the radii of gyration for the axial and circumferential directions. Thus

$$\gamma = 1.0 - 0.901 \, (1 - e^{-\phi}) \tag{32}$$

where

$$\phi = \frac{1}{29.8} \left[\frac{r}{\sqrt[4]{\frac{\overline{D}_x \overline{D}_y}{\overline{E}_x \overline{E}_y}}} \right]^{1/2} . \tag{33}$$

3.1.2.2 Bending.

Theoretical and experimental results [10, 20-23], indicate that the critical maximum load per unit circumference of a stiffened cylinder

in bending can exceed the critical unit load in axial compression. In the absence of an extensive investigation, it is recommended that the critical maximum load per unit circumference of a cylinder with closely spaced stiffeners be taken as equal to the critical load in axial compression, which is calculated from equation (24) multiplied by a factor of 0.75.

For layered or unstiffened orthotropic cylinders with negligible coupling coefficients, it is recommended that the maximum unit load be calculated by equation (31) with γ replaced by

$$\gamma = 1.0 - 0.731\ (1-e^{-\phi}) \tag{34}$$

where

$$\phi = \frac{1}{29.8}\left[\frac{r}{\sqrt[4]{\frac{\bar{D}_x\,\bar{D}_y}{\bar{E}_x\,\bar{E}_y}}}\right]^{1/2} \tag{35}$$

3.1.2.3 External Pressure.

The counterpart of equation (24) for stiffened orthotropic cylinders under lateral pressure is given by

$$p = \frac{r}{n^2}\,\frac{\begin{vmatrix} A_{11} & A_{12} & A_{13} \\ A_{21} & A_{22} & A_{23} \\ A_{31} & A_{32} & A_{33} \end{vmatrix}}{\begin{vmatrix} A_{11} & A_{12} \\ A_{21} & A_{22} \end{vmatrix}} \tag{36}$$

For hydrostatic pressure, the quantity n^2 shown in equation (36) is replaced by

$$n^2 + 1/2 \left(\frac{m \pi r}{\ell}\right)^2 \quad .$$

In the case of lateral pressure, m is equal to unity, whereas n must be varied to yield a minimum value of the critical pressure but not less than 2. In the case of hydrostatic pressure, the value of m should be varied as well as n. For long cylinders, equation (36) is replaced by

$$p = \frac{3\left(\overline{D}_y - \frac{\overline{D}_y^2}{\overline{E}_y}\right)}{r^3} \quad . \tag{37}$$

If the coupling coefficients $\overline{C}_x$, $\overline{C}_y$, $\overline{C}_{xy}$, and $\overline{K}_{xy}$ can be neglected, the critical buckling pressure can be approximated by [24]:

$$p \approx \frac{5.513}{\ell r^{3/2}} \left[\frac{\overline{D}_y^3\left(\overline{E}_x \overline{E}_y - \overline{E}_{xy}^2\right)}{\overline{E}_y}\right]^{1/4} \tag{38}$$

for

$$\left(\frac{\overline{D}_y}{\overline{D}_x}\right)^{3/2} \left(\frac{\overline{E}_x \overline{E}_y - \overline{E}_{xy}^2}{12\, \overline{E}_y \overline{D}_x}\right)^{1/2} \frac{\ell^2}{r} > 500 \quad . \tag{39}$$

Equation (36) has been investigated primarily for isotropic cylinders with ring stiffeners [25-27]. For closely spaced ring stiffening, References 25 and 26 show that the effectiveness of inside or outside rings depends on the shell and ring geometries. Generally, for shells with values of Z less than 100, outside rings are more effective than inside rings, whereas for values of Z greater than 500, the reverse is true. As the ring geometry varies, the effectiveness of outside stiffening tends to increase as the stiffness of the rings relative to the shell increases. Somewhat lower buckling pressures are given by the extremely complex but more accurate theory of Reference 28, but the differences are not so significant as to warrant its use.

The experimental results for ring-stiffened cylinders described in Reference 29 are in reasonably good agreement with the theoretical results of equation (36). However, for cylinders of all types, it is recommended that the buckling pressure calculated from equation (36) be multiplied by a factor of 0.75 for use in design, as has been recommended for unstiffened isotropic cylinders of moderate length.

3.1.2.4 Torsion.

The problem of torsional buckling of orthotropic cylinders has been treated in References 24 and 30, which do not take into account coupling between bending and extension, and in Reference 31, which does. If coupling effects are negligible, the critical torque of moderately long cylinders can be estimated from the relationship [24]:

$$M_t \approx 21.75\, \bar{D}_y^{5/8} \left(\frac{\bar{E}_x \bar{E}_y - \bar{E}_{xy}^2}{\bar{E}_y} \right)^{3/8} \frac{r^{5/4}}{\ell^{1/4}} \qquad (40)$$

for

$$\left(\frac{\bar{D}_y}{\bar{D}_x}\right)^{5/6}\left(\frac{\bar{E}_x\bar{E}_y-\bar{E}_{xy}^2}{12\,\bar{E}_y\bar{D}_x}\right)^{1/2}\frac{\ell^2}{r}\geq 500 \quad . \tag{41}$$

Reference 31, however, shows that coupling effects are quite important for cylinders stiffened by closely spaced rings. For long shells internal rings are generally more effective than outside rings; for short shells the reverse is true. In the absence of general formulas or graphs to cover the entire range of parameters that should be considered, the equations of Reference 31 should be solved for each specific case considered.

The test data of Reference 32 are in good agreement with theoretical predictions but are insufficient to provide an adequate test of the theory. It is therefore recommended that theoretical critical torques be multiplied by a factor of 0.67 for moderately long cylinders.

3.1.2.5 Combined Bending and Axial Compression.

On the basis of theory [10, 20, 21] and limited experimental data [9-10], a straight-line interaction curve is recommended for orthotropic cylinders subjected to combined bending and axial compression. The critical combinations of loading are thus given by

$$R_c + R_b = 1 \quad . \tag{42}$$

3.1.2.6 Elastic Constants.

The values of the various elastic constants used in the theory of buckling of orthotropic cylinders are different for different types of construction.

I. Stiffened Multilayered Orthotropic Cylinders.

Some widely used expressions for this type of cylinder are:

$$\overline{E}_x = \sum_{k=1}^{N} \left(\frac{E_x}{1 - \mu_x \mu_y} \right)_k t_k + \frac{E_s A_s}{b} \quad . \tag{43}$$

$$\overline{E}_y = \sum_{k=1}^{N} \left(\frac{E_y}{1 - \mu_x \mu_y} \right)_k t_k + \frac{E_r A_r}{d} \quad . \tag{44}$$

$$\overline{E}_{xy} = \sum_{k=1}^{N} \left(\frac{\mu_x E_y}{1 - \mu_x \mu_y} \right)_k t_k = \sum_{k=1}^{N} \left(\frac{\mu_y E_x}{1 - \mu_x \mu_y} \right)_k t_k \quad . \tag{45}$$

$$\overline{G}_{xy} = \sum_{k=1}^{N} \left(G_{xy} \right)_k t_k \quad . \tag{46}$$

$$\overline{D}_x = \sum_{k=1}^{N} \left(\frac{E_x}{1 - \mu_x \mu_y} \right)_k \left(\frac{1}{12} t_k^3 + t_k \tilde{z}_k^2 \right) + \frac{E_s I_s}{b} + \tilde{z}_s^2 \frac{E_s A_s}{b} \quad . \tag{47}$$

$$\overline{D}_y = \sum_{k=1}^{N} \left(\frac{E_y}{1 - \mu_x \mu_y} \right)_k \left(\frac{1}{12} t_k^3 + t_k \tilde{z}_k^2 \right) + \frac{E_r I_r}{b} + \tilde{z}_r^2 \frac{E_r A_r}{d} \quad , \tag{48}$$

$$\overline{D}_{xy} = \sum_{k=1}^{N} \left(4G_{xy} + \frac{\mu_x E_y}{1 - \mu_x \mu_y} + \frac{\mu_y E_x}{1 - \mu_x \mu_y} \right)_k \frac{1}{12} t_k^3 + t_k \tilde{z}_k^2 + \frac{G_s J_s}{b} + \frac{G_r J_r}{d} \quad , \tag{49}$$

$$\overline{C}_x = \sum_{k=1}^{N} \left(\frac{E_x}{1 - \mu_x \mu_y} \right)_k t_k \tilde{z}_k + \tilde{z}_s \frac{E_s A_s}{b} \quad , \tag{50}$$

$$\overline{C}_y = \sum_{k=1}^{N} \left(\frac{E_y}{1 - \mu_x \mu_y} \right)_k t_k \tilde{z}_k + \tilde{z}_r \frac{E_r A_r}{d} \quad , \tag{51}$$

$$\overline{C}_{xy} = \sum_{k=1}^{N} \left(\frac{\mu_y E_x}{1 - \mu_x \mu_y} \right)_k t_k \tilde{z}_k = \sum_{k=1}^{N} \left(\frac{\mu_x E_y}{1 - \mu_x \mu_y} \right)_k t_k \tilde{z}_k \quad , \tag{52}$$

$$\overline{K}_{xy} = \sum_{k=1}^{N} \left(G_{xy} \right)_k t_k \tilde{z}_k \quad , \tag{53}$$

where the subscript k refers to the material and geometry of the k^{th} layer of an N-layered shell (Fig. 3.1-6). A proper choice of the reference surface can make at least one of the coupling coefficients vanish. For example, if Δ is taken as

$$\Delta = \frac{\sum_{k=1}^{N} \left(\frac{\mu_y E_x}{1 - \mu_x \mu_y} \right)_k t_k \delta_k}{\overline{E}_{xy}} \quad , \tag{54}$$

the coefficient $\overline{C}_{xy}$ vanishes, and if

$$\Delta = \frac{\sum_{k=1}^{N} \left(G_{xy} \right)_k t_k \delta_k}{\overline{G}_{xy}} \quad , \tag{55}$$

the coefficient $\overline{K}_{xy}$ vanishes.

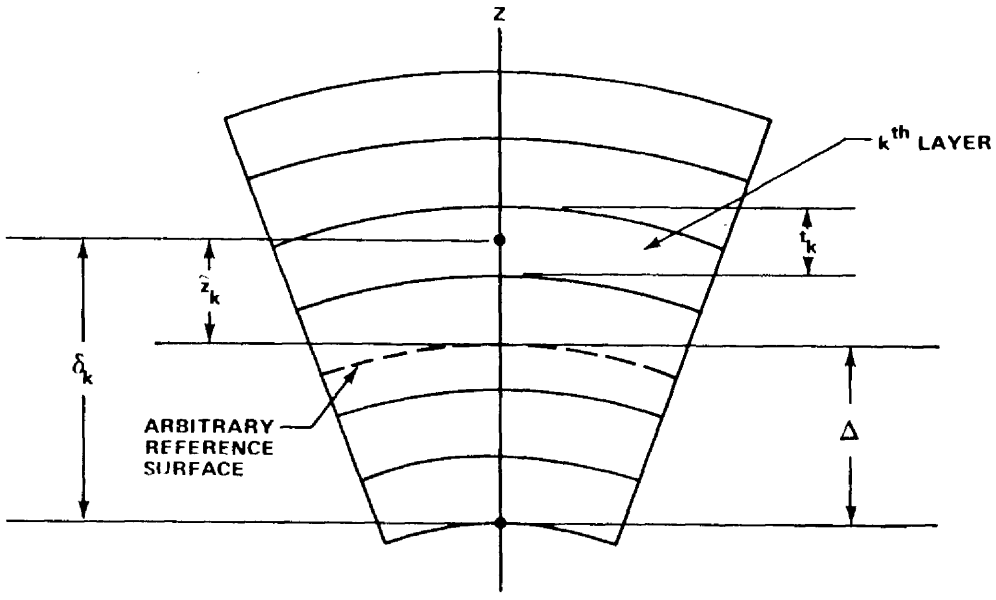

FIGURE 3.1-6. MULTILAYERED ORTHOTROPIC CYLINDRICAL SHELL GEOMETRY

II. Isotropic Cylinders with Stiffeners and Rings.

For a cylinder consisting of a stiffened single isotropic layer and for a reference surface at the center of the layer, equations (43) to (53) reduce to

$$\overline{E}_x = \frac{Et}{1-\mu^2} + \frac{E_s A_s}{b} \quad . \tag{56}$$

$$\overline{E}_y = \frac{Et}{1-\mu^2} + \frac{E_r A_r}{d} \quad . \tag{57}$$

$$\overline{E}_{xy} = \frac{\mu Et}{1-\mu^2} \quad . \tag{58}$$

$$\overline{G}_{xy} = \frac{Et}{2(1+\mu)} \quad . \tag{59}$$

$$\overline{D}_x = \frac{Et^3}{12(1-\mu^2)} + \frac{E_s I_s}{b} + \tilde{z}_s^2 \frac{E_s A_s}{b} \quad . \tag{60}$$

$$\overline{D}_y = \frac{Et^3}{12(1-\mu^2)} + \frac{E_r I_r}{d} + \tilde{z}_r^2 \frac{E_r A_r}{d} \quad . \tag{61}$$

$$\overline{D}_{xy} = \frac{Et^3}{6(1+\mu)} + \frac{G_s J_s}{b} + \frac{G_r J_r}{d} \quad . \tag{62}$$

$$\overline{C}_x = \tilde{z}_s \frac{E_s A_s}{b} \quad . \tag{63}$$

$$\overline{C}_y = \tilde{z}_r \frac{E_r A_r}{d} \quad . \tag{64}$$

$$\overline{C}_{xy} = \overline{K}_{xy} = 0 \quad . \tag{65}$$

III. Ring-Stiffened Corrugated Cylinders.

The following formulas are commonly used to calculate the required stiffnesses of ring-stiffened corrugated cylinders, with the choice of formula depending on the different assumptions which may be made:

$$\overline{E}_x = E\overline{t}\ , \ \overline{E}_y = \frac{E_r A_r}{d} \quad , \tag{66}$$

$$\overline{G}_{xy} = Gt\left(\frac{t}{\overline{t}}\right) \quad . \tag{67}$$

$$\overline{D}_x = E\overline{I} \quad . \tag{68}$$

$$\overline{D}_y = \frac{E_r I_r}{d} + \tilde{z}_r^2 \frac{E_r A_r}{d} \quad . \tag{69}$$

$$\overline{D}_{xy} = \frac{G_r J_r}{d} \quad . \tag{70}$$

$$\overline{C}_y = \tilde{z}_r \frac{E_r A_r}{d} \quad . \tag{71}$$

$$\overline{E}_{xy} = \overline{C}_{x} = \overline{C}_{xy} = \overline{K}_{xy} = 0 \qquad (72)$$

Slightly different stiffnesses are given in Reference 22.

IV. Waffle-Stiffened Cylinders.

Stiffnesses for cylinders with waffle-like walls are described in References 33 to 35.

V. Special Considerations.

In some designs of stiffened cylinders, the skin may buckle before failure of the cylinder. Buckled sheet is less stiff than unbuckled sheet. The decreased stiffness can be calculated by methods similar to those presented in References 13, 23, and 36.

3.1.3 ISOTROPIC SANDWICH CYLINDERS.

The term "isotropic sandwich" designates a layered construction formed by bonding two thin facings to a thick core. Generally, the thin facings provide nearly all the bending rigidity of the construction. The core separates the facings and transmits shear so that the facings bend about a neutral axis. The core provides the shear rigidity of the sandwich construction.

Sandwich construction should be checked for two possible modes of instability failure: (1) general instability failure where the shell fails with core and facings acting together, and (2) local instability taking the form of dimpling of the faces or wrinkling of the faces (Fig. 3.1-7).

If the isotropic sandwich shell has thin facings and the core has relatively little bending stiffness, then for unequal thickness facings the bending stiffness is given by

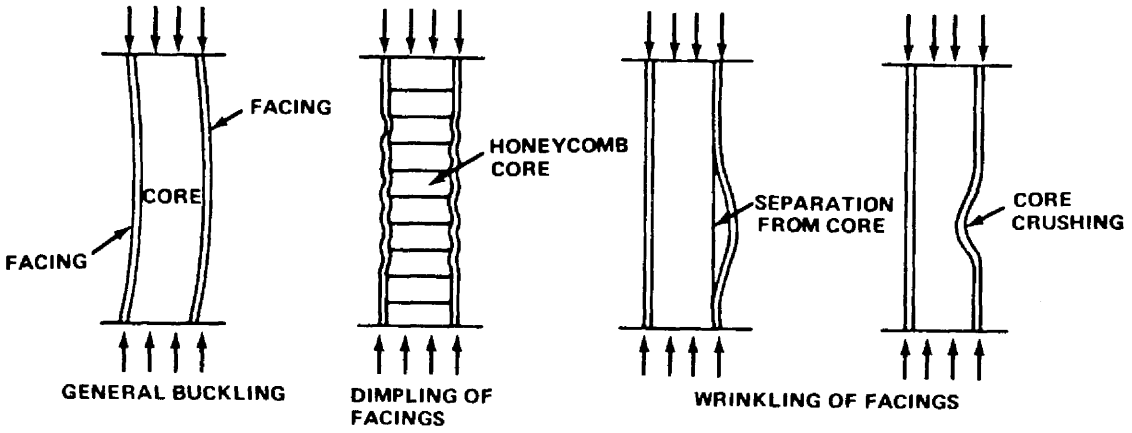

FIGURE 3.1-7. TYPES OF FAILURE OF SANDWICH SHELLS

$$D_1 = \frac{E t_1 t_2 h^2}{(1 - \mu^2)(t_1 + t_2)} \tag{73}$$

and for equal thickness facings,

$$D_1 = \frac{E t_f h^2}{2(1 - \mu^2)} \tag{74}$$

The extensional stiffness for unequal thickness facings is given by

$$B_1 = \frac{E}{(1 - \mu^2)} (t_1 + t_2) \tag{75}$$

and for equal thickness,

$$B_1 = \frac{2 E t_f}{(1 - \mu^2)} \tag{76}$$

The transverse shear stiffness for an isotropic core is given by

$$D_q = G_{xz} \frac{h^2}{h - \frac{t_1 + t_2}{2}} \tag{77}$$

and for equal thickness,

$$D_q = G_{xz} \frac{h^2}{h - t_f} \tag{78}$$

The stiffness of other types of sandwich construction is given in References 37, 38, and 39.

3.1.3.1 Axial Compression.

Investigations of the buckling behavior of isotropic sandwich circular cylinders in axial compression are reported in References 40 and 41. Design information from these references is given in Figures 3.1-8 and 3.1-9.

Figure 3.1-9 is the more convenient of the two figures to use and is applicable to all but unusually short cylinders [$\gamma Z < \pi^2/(1 + R)$]. Figures 3.1-8 and 3.1-9 are based on the small-deflection buckling theory and should be used in conjunction with the correlation factor of Figure 3.1-10 to predict buckling loads. Figure 3.1-10 is based on equation (32), given for orthotropic cylinders. For the present application the parameter ϕ becomes

$$\phi = \frac{\sqrt{2}}{29.8} \sqrt{\frac{r}{h}} \tag{79}$$

This procedure is consistent with the procedures given earlier for other types of construction when shearing of the core does not contribute significantly to the buckling deformations, that is, when N_o/D_q of Figure 3.1-9 is small.

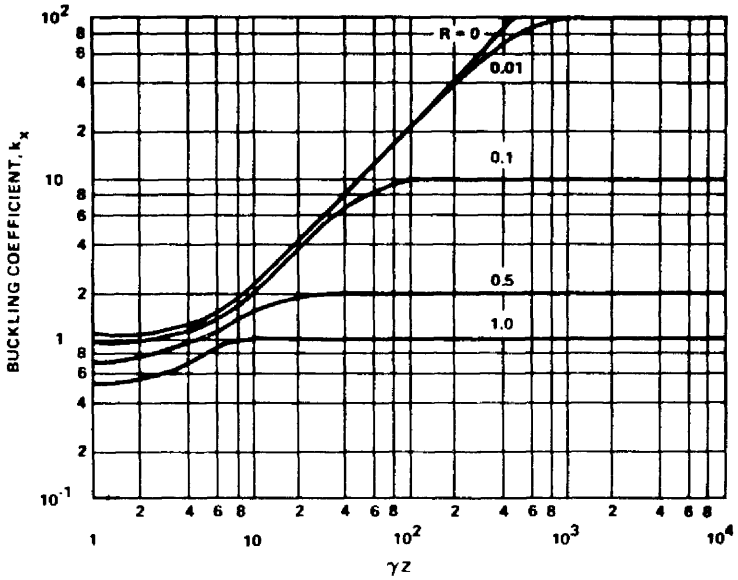

FIGURE 3.1-8. BUCKLING COEFFICIENTS FOR SIMPLY SUPPORTED ISOTROPIC SANDWICH CIRCULAR CYLINDERS SUBJECTED TO AXIAL COMPRESSION $G_{xz}/G_{yz} = 1.0$

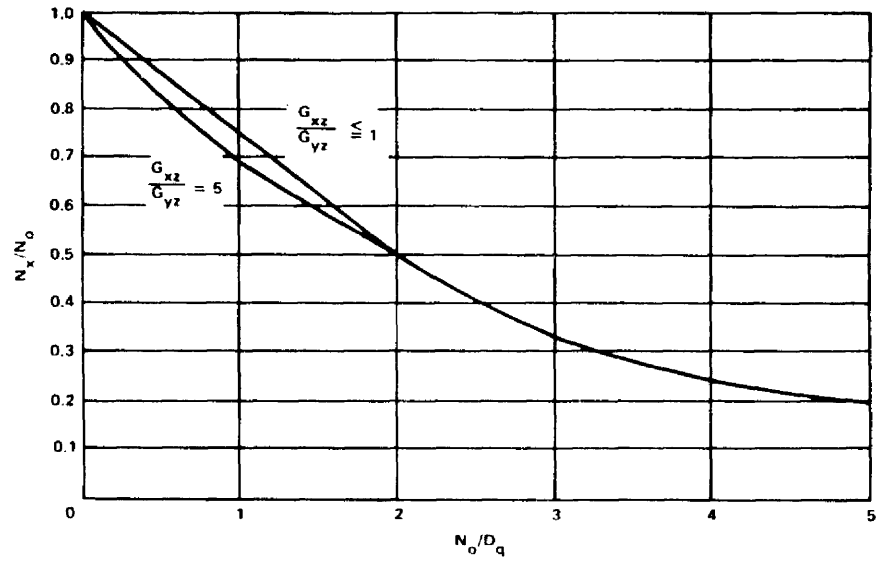

FIGURE 3.1-9. BUCKLING OF MODERATELY LONG, SIMPLY SUPPORTED, ISOTROPIC SANDWICH CIRCULAR CYLINDERS SUBJECTED TO AXIAL COMPRESSION

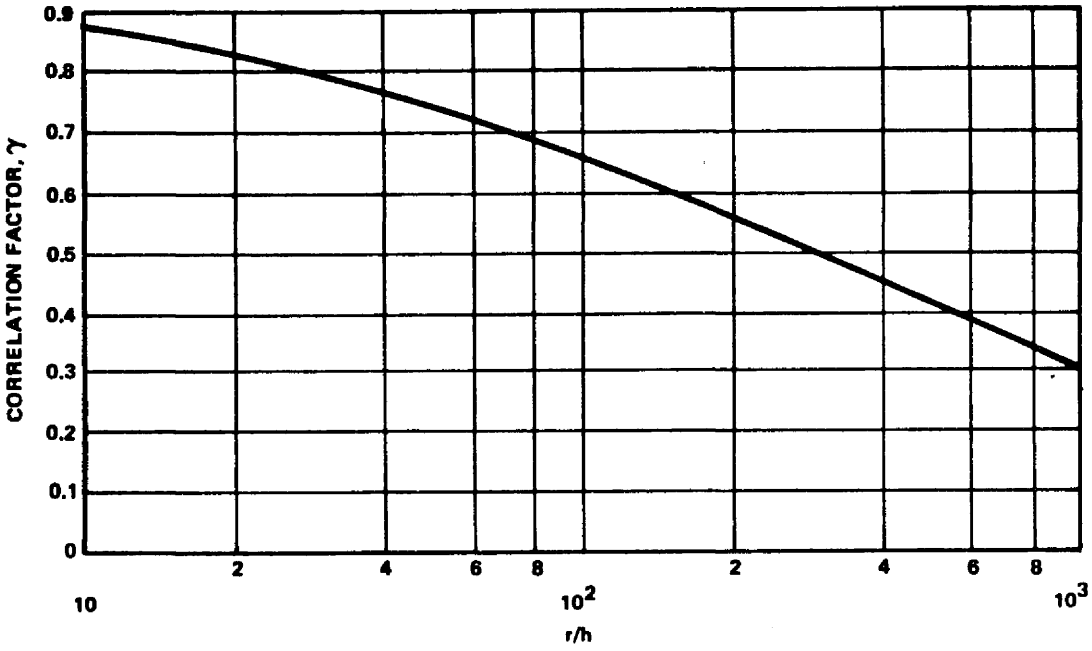

FIGURE 3.1-10. CORRELATION FACTORS FOR ISOTROPIC SANDWICH CIRCULAR CYLINDERS SUBJECTED TO AXIAL COMPRESSION

As shearing deformations become more pronounced, the correction resulting from application of the factor γ, as prescribed above, decreases and becomes zero in the limiting condition of buckling from a weak core $[(N_o/D_q) > 2]$.

A weight-strength study based on Figure 3.1-9 and published values for the shear stiffness of honeycomb cores [42] indicate that unusually lightweight cores are more desirable than heavier cores. Until adequate test data are obtained to substantiate this indication, however, designs should be limited to sandwiches with rather heavy cores ($\delta \geq 0.03$). Also, it has been found that sandwich plates with light honeycomb cores are susceptible to additional modes of deformation, and failure may result from intracell

buckling, face wrinkling, or an interaction of one or both of these modes with a cylinder-buckling mode. In addition, small buckle-like deformations have occurred in actual structures long before the theoretical buckling load was reached (see, for example, Ref. 43, p. 217). This behavior requires that the structure be capable of resisting internal moments and shears in addition to the directly applied loads. In the case of sandwich cylinders, the moments and shears may cause core buckling or shear failure of the core.

The only known method of preventing these core failures is to use relatively heavy cores which have considerable strength in crushing and shear. Honeycomb cores with a density ratio $\delta = 0.03$ should be adequate to prevent these core failures. Large margins against failure in intracell buckling and wrinkling can be obtained with rather heavy cores with little or no weight penalty. Moreover, when heavy cores are used approximate equations are adequate for predicting failures in the intracell buckling and face-wrinkling modes. The following equations may be used for this purpose. For intracell buckling:

$$\sigma_x = 2.5\, E_R\, (t/S)^2 \tag{80}$$

where S is the core cell size expressed as the diameter of the largest inscribed circle and

$$E_R = \frac{4\, E\, E_{tan}}{\left(\sqrt{E} + \sqrt{E_{tan}}\right)^2} \tag{81}$$

where E and E_{tan} are the elastic and tangent moduli of the face-sheet material. If initial dimpling is to be checked, the equation

$$\sigma_x = 2.2\, E_R\, (t/S)^2 \qquad (82)$$

should be used. The sandwich will still carry load if initial dimpling occurs.

Critical wrinkling stresses are predicted by

$$\sigma_x = 0.50\, (E_{sec}\, E_z\, G_{xz})^{1/3} \qquad (83)$$

where E_z is the modulus of the core in a direction perpendicular to the core, and G_{xz} is the shear modulus of the core in the x-z plane. If biaxial compressive stresses are applied to the sandwich, then the coefficients of the equations must be reduced by the factor $(1 + f^3)^{-1/3}$ where

$$f = \frac{\text{minimum principal compressive stress in facings}}{\text{maximum principal compressive stress in facings}} \qquad (84)$$

Wrinkling and intracell-buckling equations which consider strength of bond, strength of foundation, and initial waviness of the facings are given in References 39, 44, and 45.

The plasticity correction factor given for isotropic cylinders in axial compression also may be applied to isotropic sandwich cylinders. The factor is applicable to sandwich cylinders with stiff cores and becomes somewhat conservative as the shear stiffness of the core is decreased [46].

3.1.3.2 Bending.

The buckling equations given in Paragraph 3.1.3.1 for circular cylinders in axial compression may be used for cylinders in bending, provided that the correlation factor γ is taken from Figure 3.1-11 instead of from Figure 3.1-10. Figure 3.1-11 is based on equation (34), given earlier for orthotropic cylinders in bending.

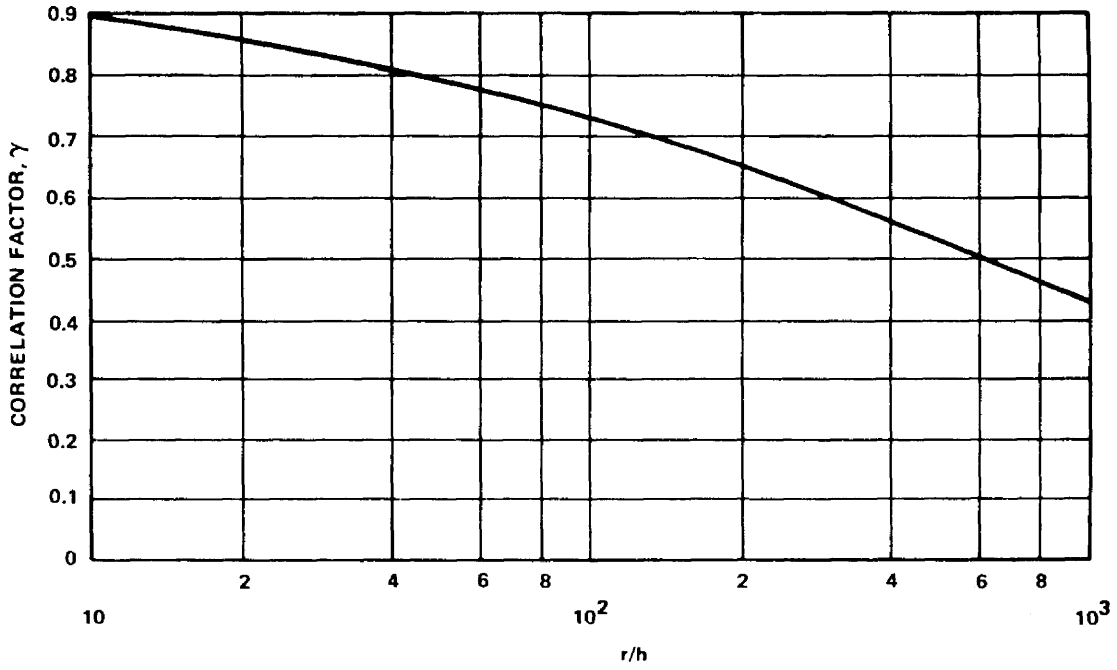

FIGURE 3.1-11. CORRELATION FACTORS FOR ISOTROPIC SANDWICH CIRCULAR CYLINDERS SUBJECTED TO BENDING

3.1.3.3 Lateral Pressure.

A plot of k_y against γZ, constructed from the data of Reference 47, is given in Figure 3.1-12. The straight-line portion of the curve of Figure 3.1-12 for a sandwich cylinder with a rigid core ($\delta=0$) is given by the equation

$$k_y = \frac{N_y \ell^2}{\pi D_1} = 0.56 \sqrt{\gamma Z} \qquad (85)$$

There are no experimental data to substantiate Figure 3.1-12. From experience with isotropic cylinders, however, it is suggested that a factor γ equal to 0.56 be used with this figure.

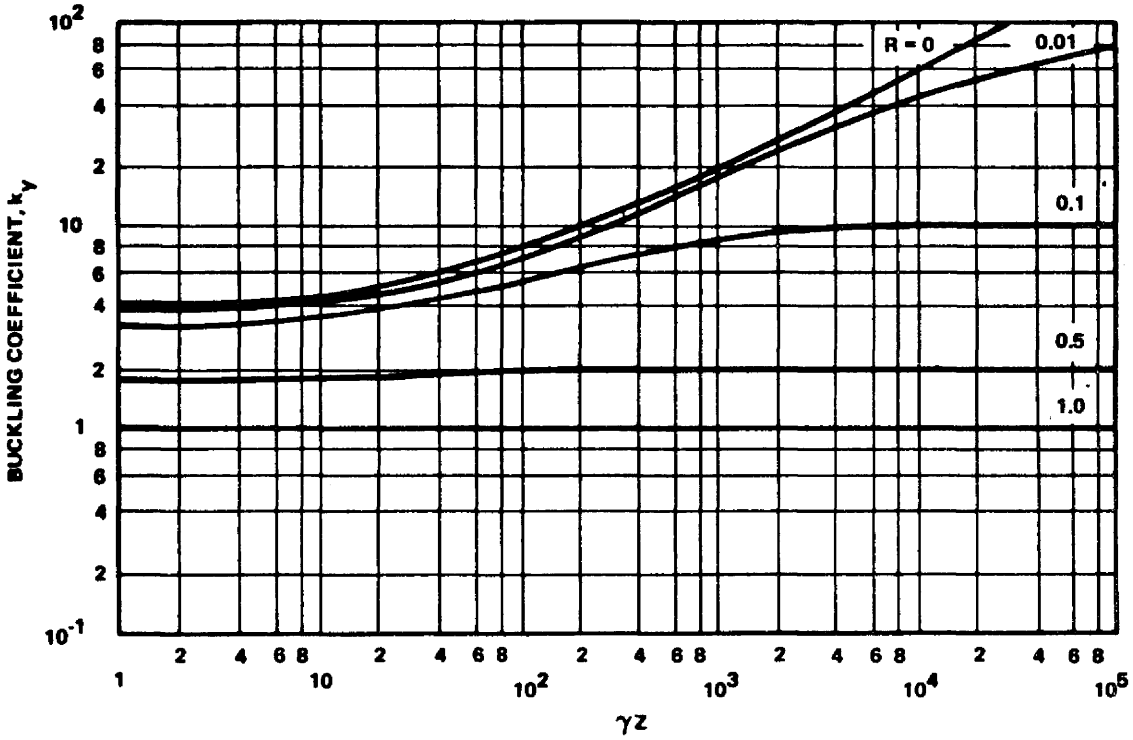

FIGURE 3.1-12. BUCKLING COEFFICIENTS FOR SIMPLY SUPPORTED ISOTROPIC SANDWICH CIRCULAR CYLINDERS SUBJECTED TO LATERAL PRESSURE $G_{xz}/G_{yz} = 1.0$

Here, as with sandwich cylinders in axial compression or bending, designs should be limited to sandwich cylinders for which the density ratio δ is 0.03 or greater, unless the design is substantiated by adequate tests.

For inelastic stresses the plasticity correction factor should be obtained from Paragraph 3.1.6. For short cylinders ($\gamma Z < 5$) the C curves should be used. For moderate-length cylinders $5 < \gamma Z < 4000$ the E_1 curve should be used. For long cylinders $\gamma Z > 4000$, the E curve should be used.

3.1.3.4 Torsion.

Isotropic sandwich cylinders in torsion have not received the same attention as cylinders in compression, although both rigid- and weak-core criteria are reasonably well defined. Whereas the transition region between

rigid and weak cores is not as well defined, the methods presented are probably sufficient for design purposes. Information on the transition region is given in References 37 and 47; the latter was used to construct the plot of Figure 3.1-13, which applies to sandwich cylinders with cores exhibiting isotropic shear behavior $G_{xz}/G_{yz} = 1$. The curves of this figure are discontinuous at the value of γZ where the buckling coefficient k_{xy} becomes equal to $1/R$, indicating a change of mode of buckling at that point.

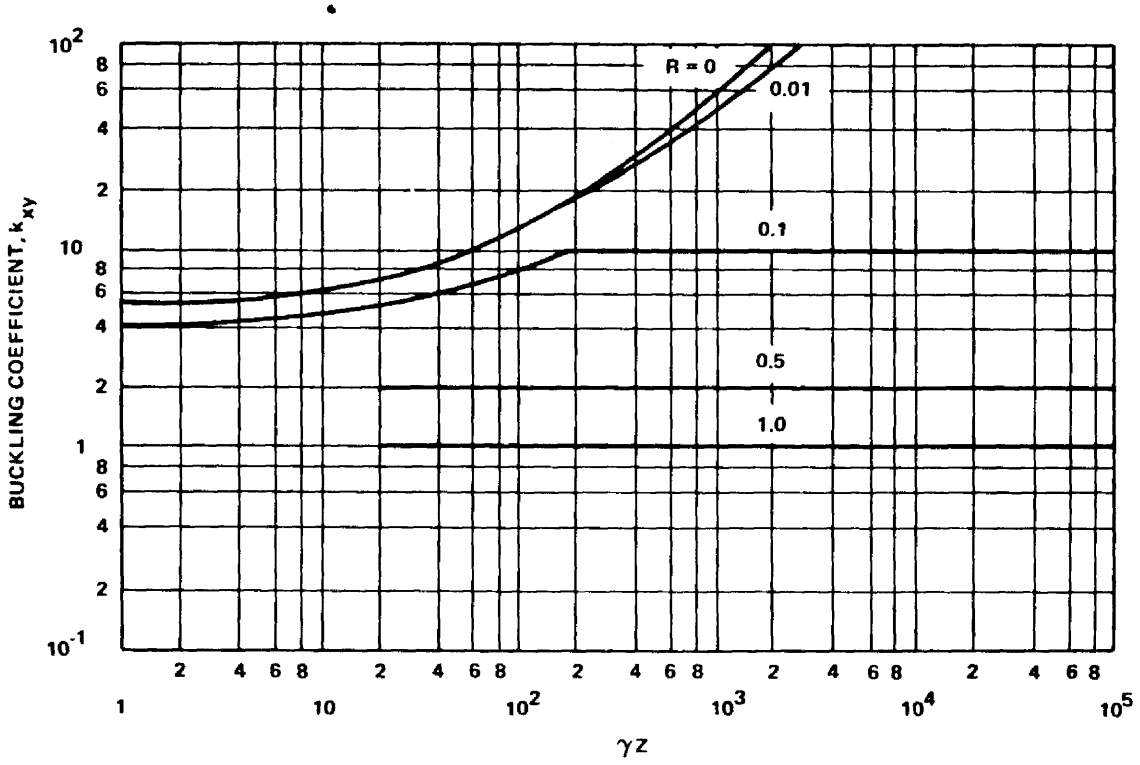

FIGURE 3.1-13. BUCKLING COEFFICIENTS FOR SIMPLY SUPPORTED ISOTROPIC SANDWICH CIRCULAR CYLINDERS SUBJECTED TO TORSION $G_{xz}/G_{yz} = 1.0$

Reference 37 does not support this behavior, but it does not cover a sufficiently wide range of geometric proportions to be used in the construction of the figure. In addition, Reference 37 indicates that there was some scatter in the calculated results used to construct the charts of that reference. In the ranges where comparisons between the data of References 37 and 47 could be made, only rather small discrepancies were noted. The straight-line portion ($\gamma Z > 170$) of the curve of Figure 3.1-13 for a rigid core ($R=0$) is given by the equation

$$k_{xy} = \frac{N_{xy}\, \ell^2}{\pi^2 D_1} = 0.34\ (\gamma Z)^{3/4} \quad . \qquad (86)$$

Experimental data are not available to substantiate Figure 3.1-13 for most sandwich cylinders. From experience with isotropic cylinders, it is indicated that 0.586 is the factor γ to be used with the figure. Here, as with sandwich cylinders for which the density ratio of δ is 0.03 or greater, the same factor should be used unless the design is substantiated by adequate tests. Plasticity may be taken into account by using the A curves of Paragraph 3.1.6.

3.1.4 CYLINDERS WITH AN ELASTIC CORE.

The term "cylinder with an elastic core" defines a thin cylindrical shell enclosing an elastic material that can be either solid or have a hole in its center. This type of shell closely approximates a propellant-filled missile structure. The propellant is generally of a viscoelastic material and therefore is strain-rate sensitive. The core modulus should be obtained from tension or compression tests of the core material simulating its expected strain rate.

Although there are some analytical data for orthotropic shells [48], design curves are given only for isotropic shells and cores. The inverse problem of a core or cushion on the outside of the cylindrical shell is analyzed in Reference 49. Not enough data are available, however, to recommend design curves for this problem.

3.1.4.1 Axial Compression.

The buckling behavior of cylindrical shells with a solid elastic core in axial compression is given in Reference 50. Analytical results obtained from this reference are shown graphically in Figure 3.1-14. For small values of ϕ_1

$$\sigma_p = (1 + \phi_1)\, \sigma_{x_{cr}} \tag{87}$$

where

$$\phi_1 = \frac{\sqrt[4]{12\,(1-\mu^2)}}{4\,(1-\mu_c^2)}\ \frac{E_c}{E}\ \left(\frac{r}{t}\right)^{3/2} \tag{88}$$

and $\sigma_{x_{cr}}$ is the critical value of axial compression for an isotropic circular cylinder, as found in Paragraph 3.1.1.1. This approximation is accurate for ϕ_1 less than one-half. For larger values of ϕ_1, for example, ϕ_1 greater than 3,

$$\sigma_p \approx 3/2\, \phi_1^{3/2}\, \sigma_{x_{cr}} \tag{89}$$

The plasticity correlation factors should be determined as in Paragraph 3.1.1.1.

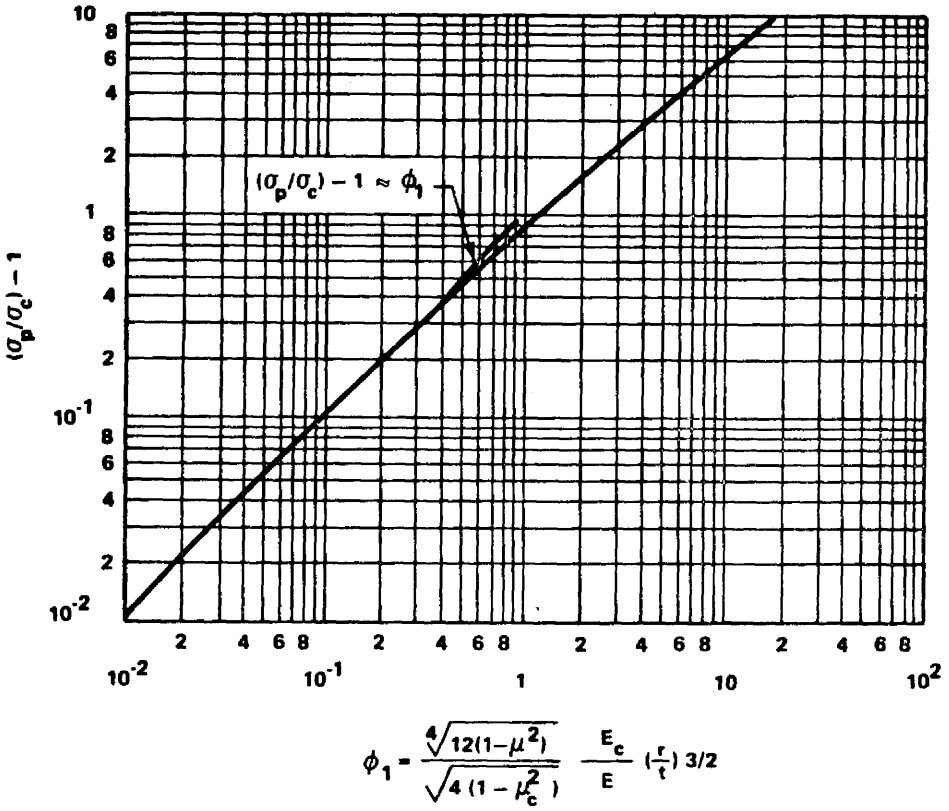

FIGURE 3.1-14. VARIATION OF COMPRESSIVE BUCKLING STRESS WITH CORE STIFFNESS PARAMETER

3.1.4.2 External Pressure.

Analytical curves for the lateral pressure core are presented in Reference 50. A plot of k_{pc} against $\frac{\pi r}{\ell}$ for $\frac{r}{t}$ = 100, 200, 500, or 1000 is shown graphically in Figure 3.1-15. The parameter k_{pc} is expressed by

$$k_{pc} = \frac{pr^3}{D} \qquad (90)$$

These curves are to be used for finite cylinders loaded by lateral pressures.

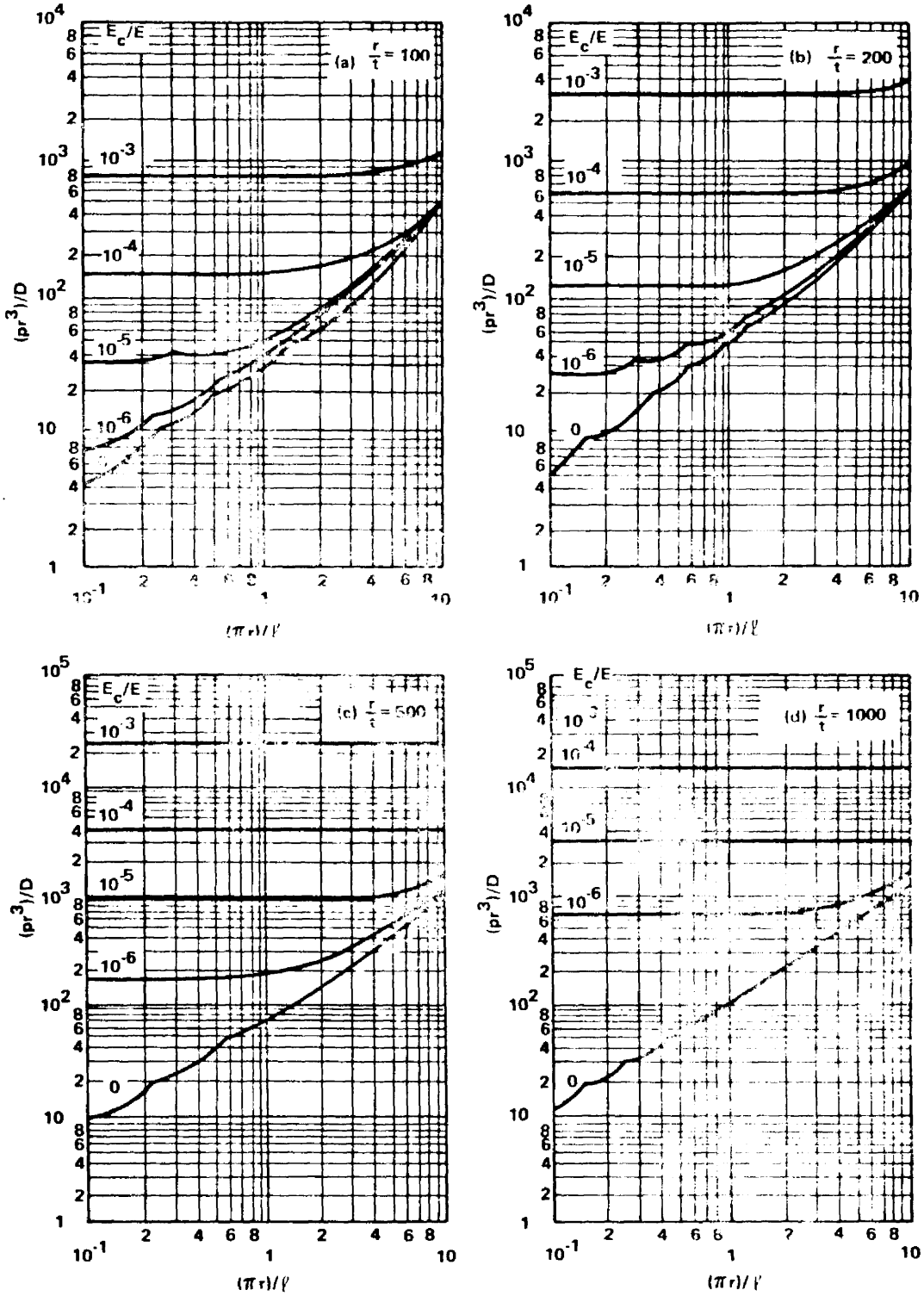

FIGURE 3.1-15. VARIATION OF BUCKLING PRESSURE COEFFICIENT WITH LENGTH AND MODULUS RATIO ($\mu = 0.3$, $\mu_c = 0.5$)

Some cylinders are long enough for the critical pressure to be independent of length; the single curve shown in Figure 3.1-16 can then be used. The straight-line portion of the curve can be approximated by the equation

$$\frac{k_{pc}}{1 + \frac{E_c r}{Et\,(1 - \mu_c)}} = 3\,(\phi_2)^{3/2} \qquad (91)$$

where

$$\phi_2 = \frac{3\,(1 - \mu^2)}{1 - \mu_c^2}\ \frac{E_c}{E}\ \left(\frac{r}{t}\right)^3 \qquad (92)$$

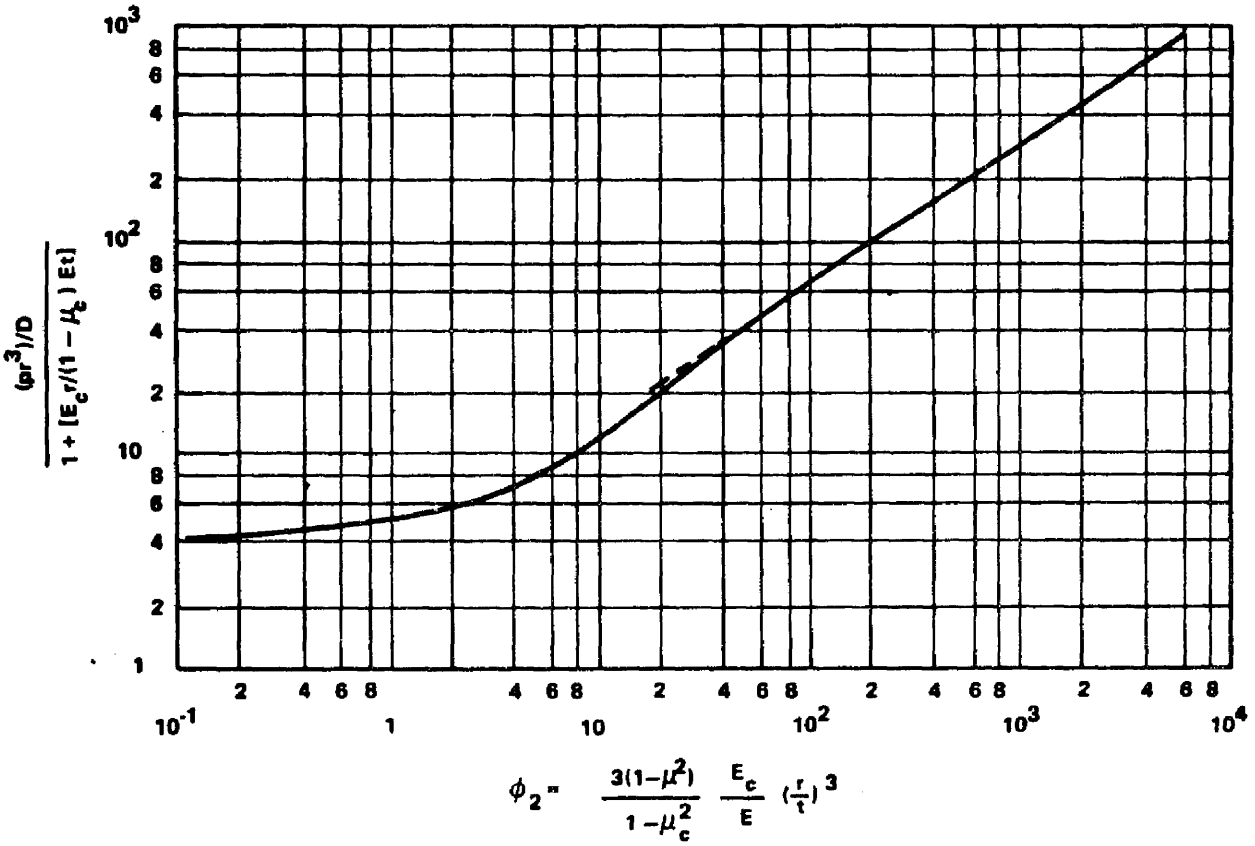

FIGURE 3.1-16. BUCKLING PRESSURE COEFFICIENTS FOR LONG CYLINDER WITH A SOLID CORE

The few experimental data points available indicate good agreement between analysis and experiment, but one test point falls 4 percent below theory. Hence, a correlation factor of 0.90 is recommended for use in conjunction with the curves in Figures 3.1-15 and 3.1-16. A reinvestigation of the factor may be warranted as more data become available. Plasticity should be accounted for by using curves A in Paragraph 3.1-6.

3.1.4.3 Torsion.

The buckling behavior of cylindrical shells with an elastic core is analytically described in Reference 51 and is shown graphically in Figure 3.1-17.

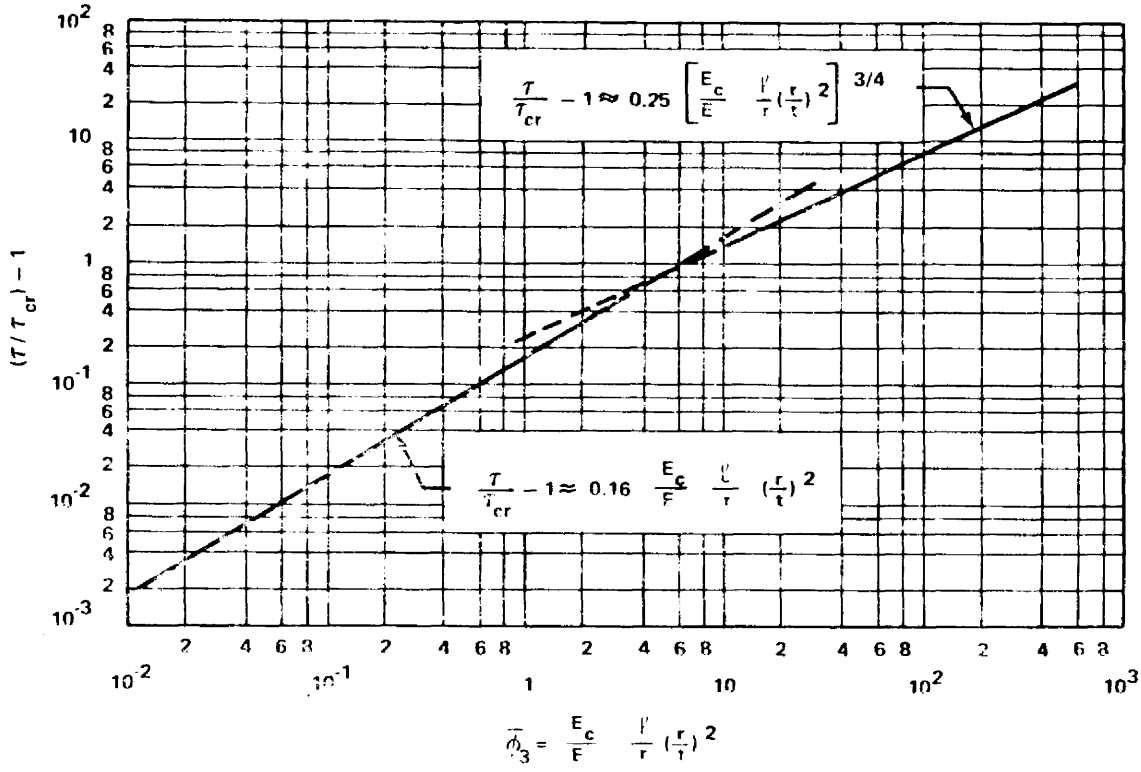

FIGURE 3.1-17. TORSIONAL BUCKLING COEFFICIENTS FOR CYLINDERS WITH AN ELASTIC CORE

For small values of ϕ_3 ($\phi_3 < 7$), the analytical results can be approximated by

$$\frac{\tau}{\tau_{xy_{cr}}} = 1 + 0.16\,\phi_3 \tag{93}$$

where

$$\phi_3 = \frac{E_c}{E}\left(\frac{\ell}{r}\right)\left(\frac{r}{t}\right)^2 \tag{94}$$

and $\tau_{xy_{cr}}$ is the torsional buckling stress given by equation (16), with γ equal to unity. When ϕ_3 is greater than 10, the analytical results follow the curve

$$\frac{\tau}{\tau_{xy_{cr}}} = 1 + 0.25\,(\phi_3)^{3/4} \tag{95}$$

Experimental data are not available for this loading condition. The experimental points obtained from cylinders with an elastic core for axial compression and external pressure, however, show better correlation with theory than the corresponding experimental results for the unfilled cylinder. Hence, conservative-design curves can be obtained by calculating $\tau_{xy_{cr}}$ in equations (93) and (95) with the correlation factor given by equation (19) and the plasticity factor given by curves A in Paragraph 3.1-6.

3.1.4.4 Combined Axial Compression and Lateral Pressure.

Interaction curves for cylinders with an elastic core subjected to combined axial compression and lateral pressure are shown in Figure 3.1-18.

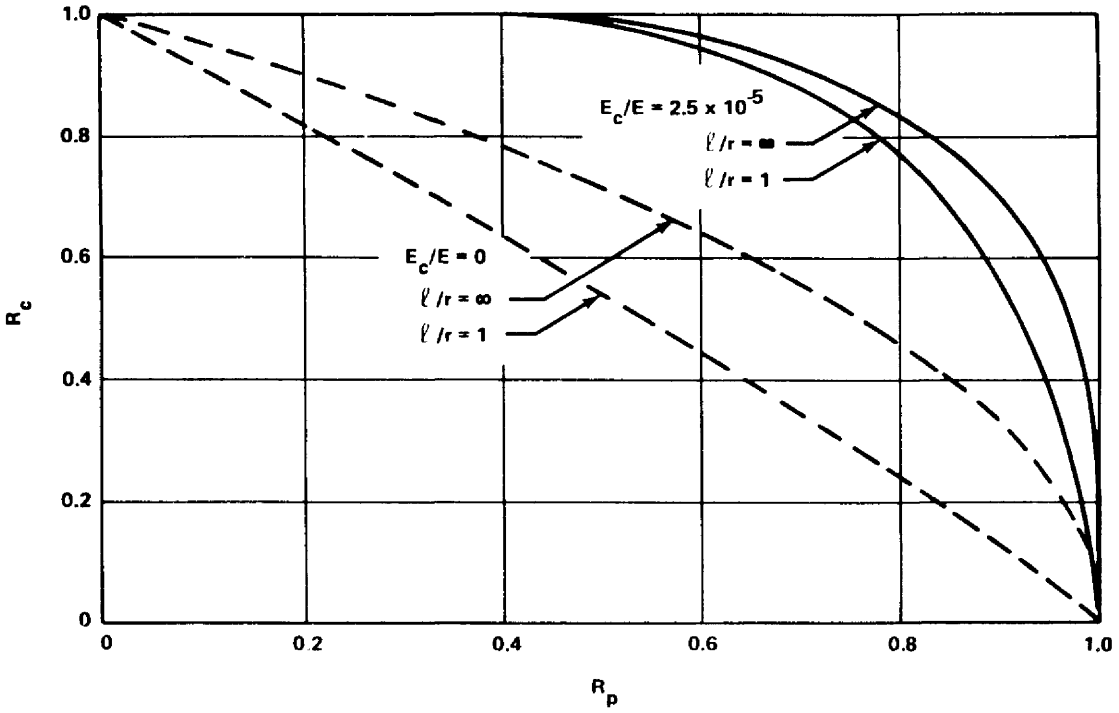

FIGURE 3.1-18. INTERACTION CURVES FOR CYLINDERS (r/t = 300) WITH AN ELASTIC CORE

These curves were obtained analytically in Reference 50 and indicate that for a sufficiently stiff core, the critical axial compressive stress is insensitive to lateral pressure, and similarly, the critical lateral pressure is insensitive to axial compression. Until more experimental data become available, the use of a straight-line interaction curve is recommended for conservative design.

3.1.5 DESIGN OF RINGS.

Little information is available on which to base the design of rings for cylinders to exclude general instability failures. The criterion of Reference 52 is frequently cited as applicable to cylinders subjected to bending or compression. Unfortunately, this criterion is empirical and based on data from

test cylinders with proportions of little interest in contemporary design. A few checks made on cylinders in use have indicated that the criterion usually is conservative, but this may not be so in certain cases [10, 53].

A less direct procedure for designing rings may be used. It consists simply of calculating the failing load of the cylinder in the so-called general-instability mode, which involves failure of the rings, as well as calculation of the failing load of the cylinder for wall failure between rings. Both calculations are made for several ring weights. If such calculations are plotted against ring weight, the weight necessary to force failure in the desired mode can be ascertained. In addition, the amount of error in weight from uncertainties in the calculations can be judged. Presumably, there may be some interaction between failing modes; thus, somewhat heavier rings than those indicated by the calculations should be used.

This method of designing rings is, of course, applicable to all types of loading and all types of wall construction. It also has the advantage of giving the designer some feeling for the influence of the various factors which determine ring weight.

A study of References 53 and 54, which present general linear analyses of ring-stiffened isotropic cylinders in torsion and of orthotropic cylinders in compression, indicates that the recommended procedure gives the same result as general theory for all cylinders except those with a single ring dividing the cylinder into two equal bays.

3.1.6 PLASTICITY CORRECTION FACTOR.

The effect of plasticity on the buckling of shells can be accounted for by the use of the plasticity coefficient, η. This coefficient is defined by the ratio

$$\eta = \frac{\sigma_{cr}}{\sigma_e}$$

where

σ_{cr} = the actual buckling stress.

σ_e = the elastic buckling stress (the stress at which buckling would occur if the material remained elastic at any stress level).

The elastic buckling stress, therefore, is given by the equation

$$\sigma_e = \frac{\sigma_{cr}}{\eta} \quad .$$

The definition of η depends on σ_{cr}/σ_e, which is a function of the loading, the type of shell, the boundary conditions, and the type of construction. For example, the η recommended for homogeneous isotropic cylindrical shells with simply supported edges subjected to axial compression is

$$\eta = \frac{\sqrt{E_t E_s}}{E} \left[\frac{1 - \mu_e^2}{1 - \mu^2} \right]^{1/2}$$

where E_t, E_s and μ are the tangent modulus, secant modulus and Poisson's ratio, respectively, at the actual buckling stress, and μ_e is the elastic Poisson's ratio.

For a given material, temperature, and η, a chart may be prepared for σ_{cr}/η versus σ_{cr}. By first calculating the elastic buckling stress, σ_{cr}/η, the actual buckling stress σ_{cr} can be read from the chart of σ_{cr}/η versus σ_{cr}. This method eliminates an iterative procedure which would otherwise be necessary.

Figures 3.1-19 through 3.1-25 present curves of σ_{cr}/η versus σ_{cr} for some materials and temperatures commonly encountered in the aerospace industry. In many cases, the curves are so close together that they are drawn as one curve.

The η used to determine each curve is defined as follows:

Curve	η
A	E_s/E
B	$\frac{E_s}{E}\left[0.330 + 0.670\sqrt{\mu^2 + (1-\mu^2)\frac{E_t}{E_s}}\right]$
C	$\frac{E_s}{E}\left[1/2 + 1/2\sqrt{\mu^2 + (1-\mu^2)\frac{E_t}{E_s}}\right]$
D	$\frac{E_s}{E}\left[0.352 + 0.648\sqrt{\mu^2 + (1-\mu^2)\frac{E_t}{E_s}}\right]$
E	$\mu^2 E_s/E + (1-\mu^2) E_t/E$
F	$0.046 E_s/E + 0.954 E_t/E$ $(\mu = 0.33)$
G	E_t/E
E_1	$\frac{\sqrt{E_t E_s}}{E}\left[\frac{1-\mu_e^2}{1-\mu^2}\right]^{1/2}$

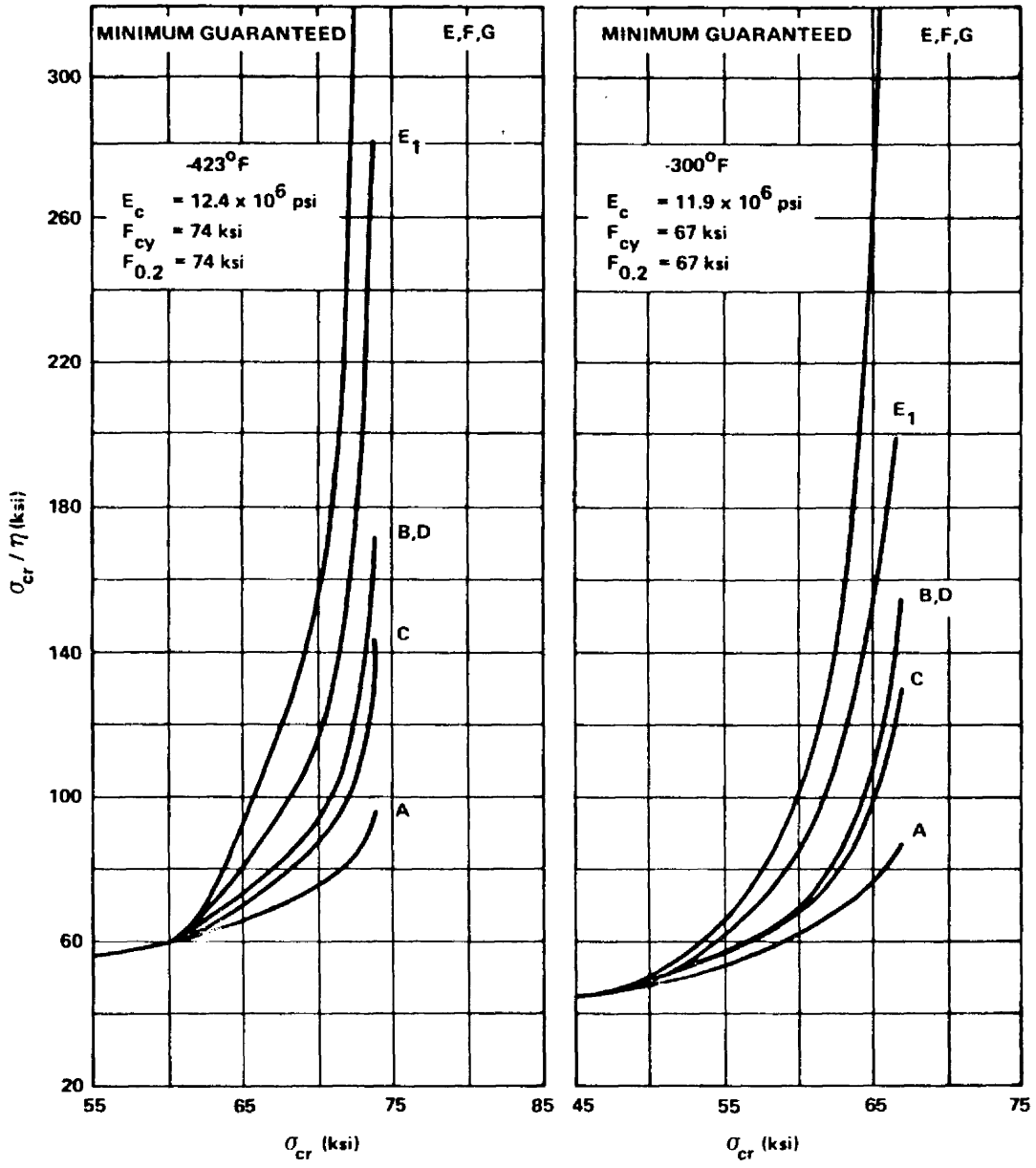

FIGURE 3.1-19. PLASTICITY CORRECTION CURVES FOR 2014-T6, -T651 ALUMINUM ALLOY SHEET AND PLATE (-423° F, -300° F)

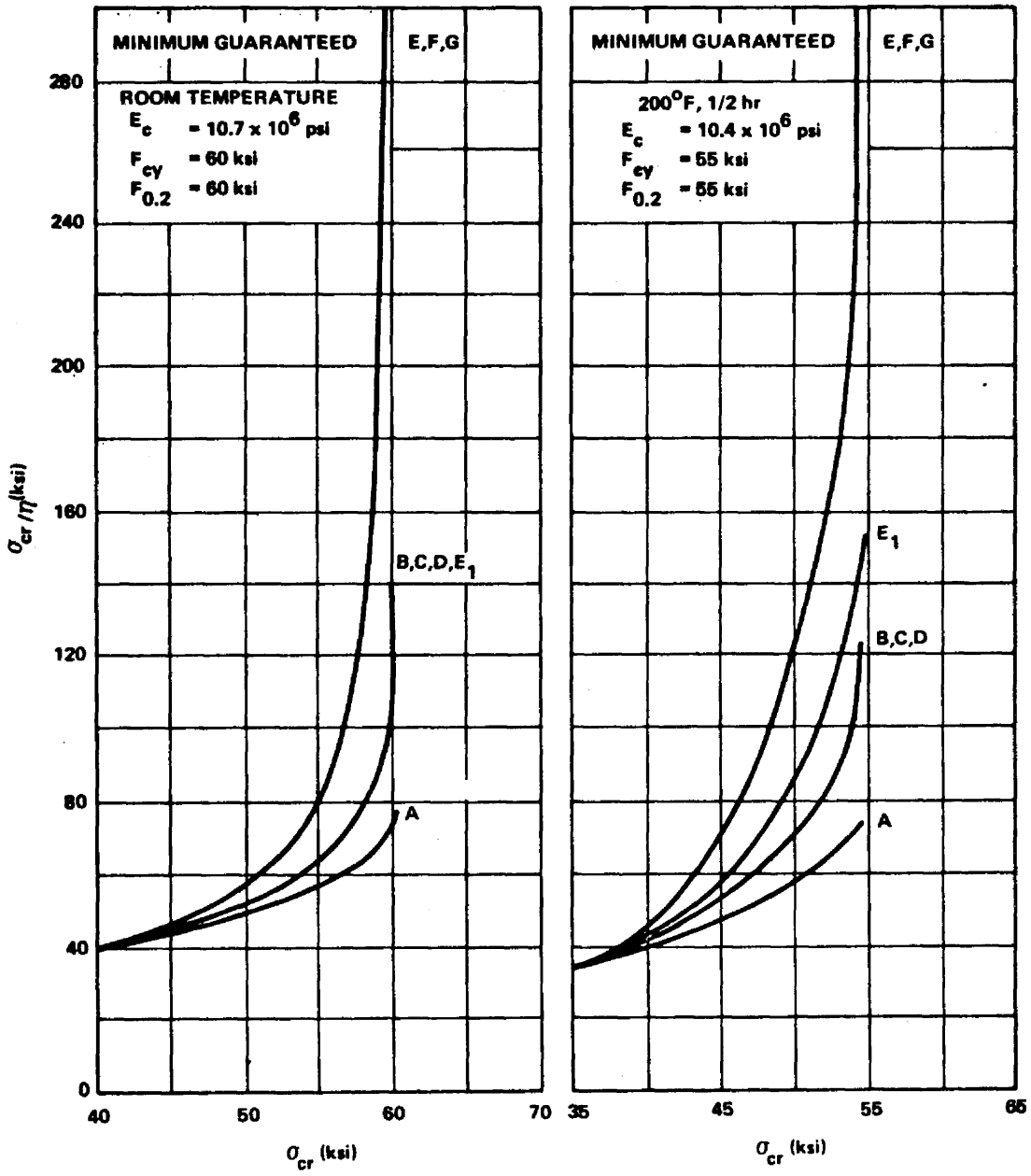

FIGURE 3.1-20. PLASTICITY CORRECTION CURVES FOR 2014-T6, -T651 ALUMINUM ALLOY SHEET AND PLATE (room temp.; 200°F, 1/2 hr)

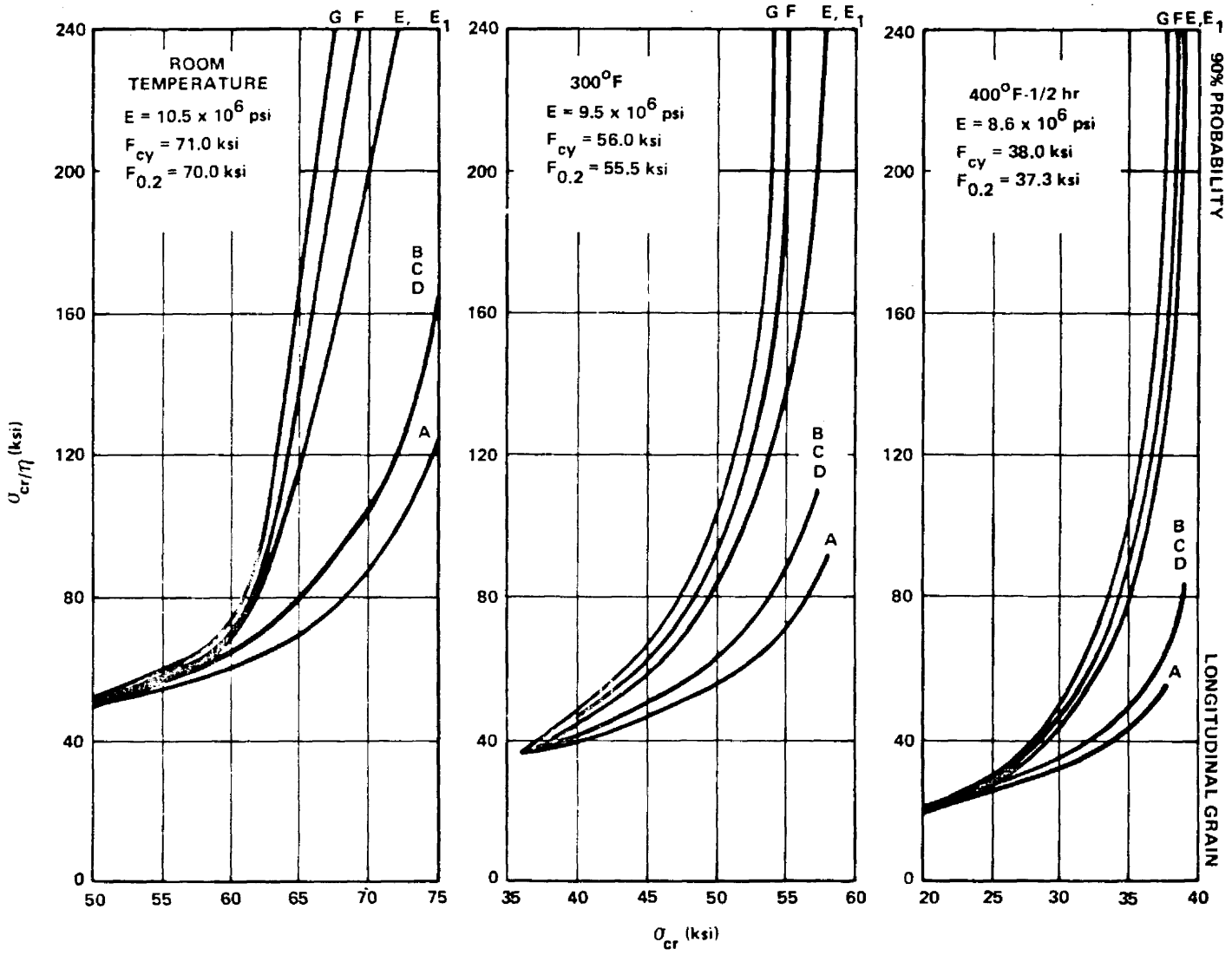

FIGURE 3.1-21. PLASTICITY CORRECTION CURVES FOR BARE 7075-T6 ALUMINUM ALLOY SHEET

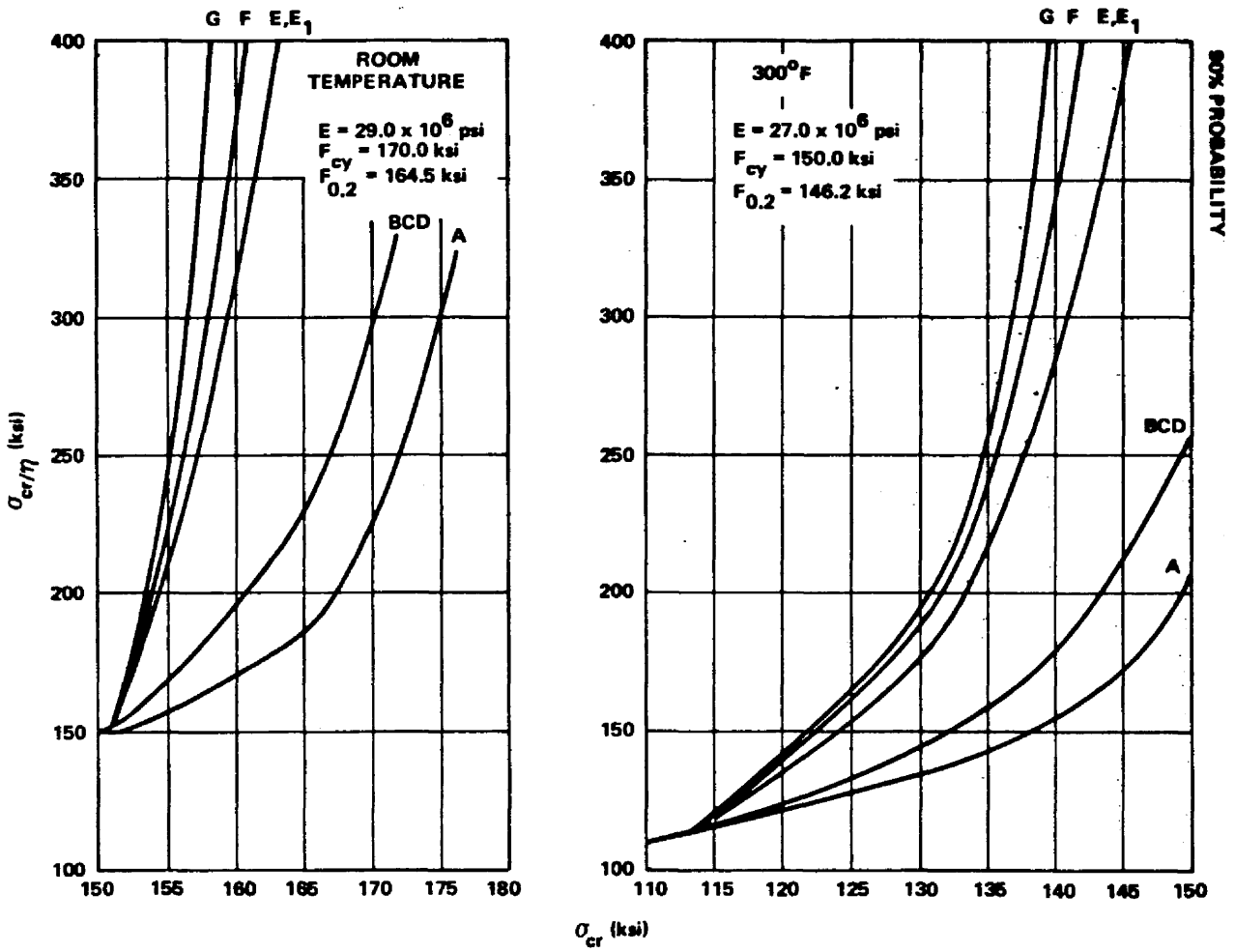

FIGURE 3.1-22. PLASTICITY CORRECTION CURVES FOR ALLOY STEEL 4130, 4140, AND 4340 (180 000 psi)

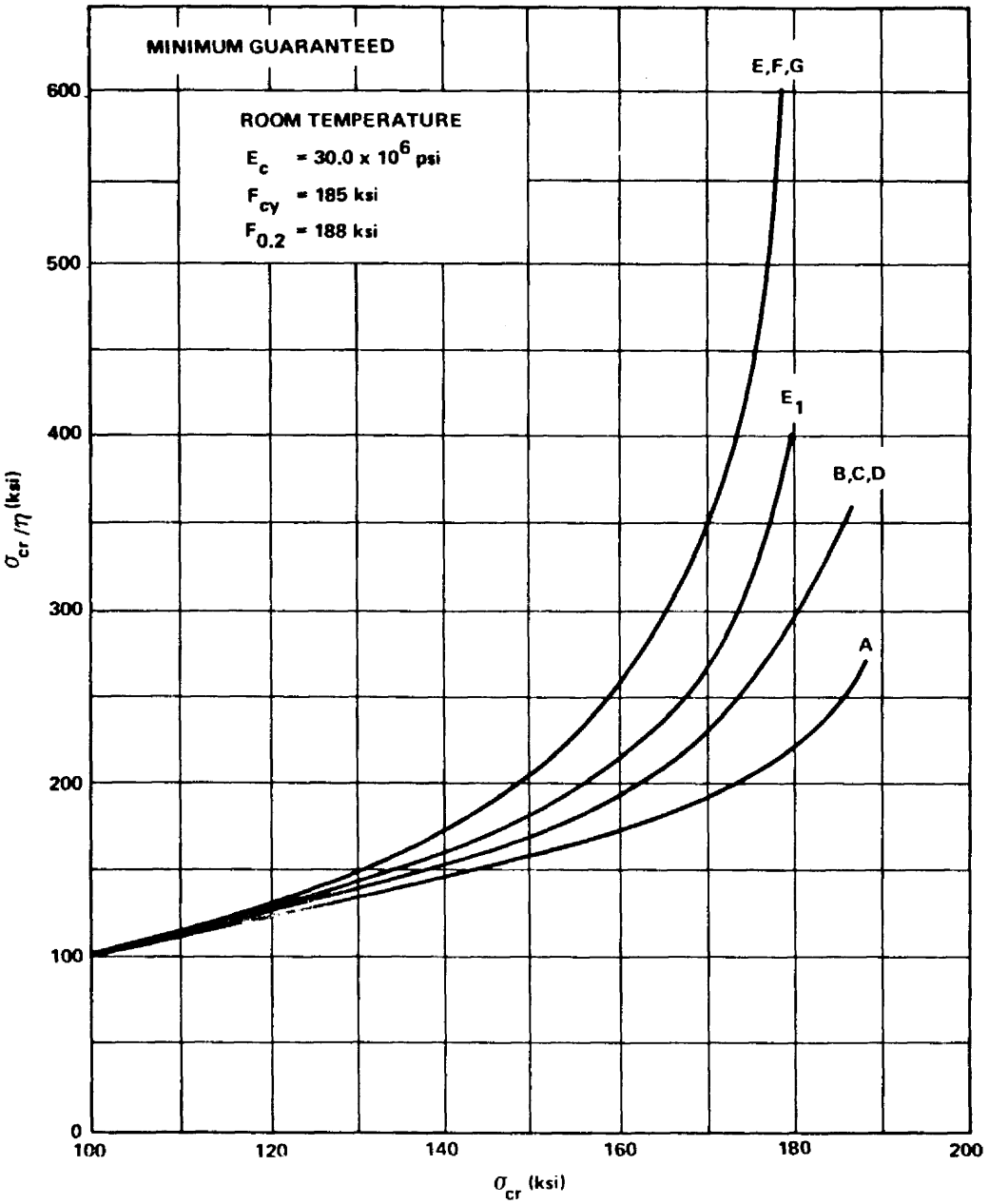

FIGURE 3.1-23. PLASTICITY CORRECTION CURVES FOR PH 15-7 Mo STAINLESS STEEL SHEET AND PLATE — RH 1050, FH 1075 (room temp.)

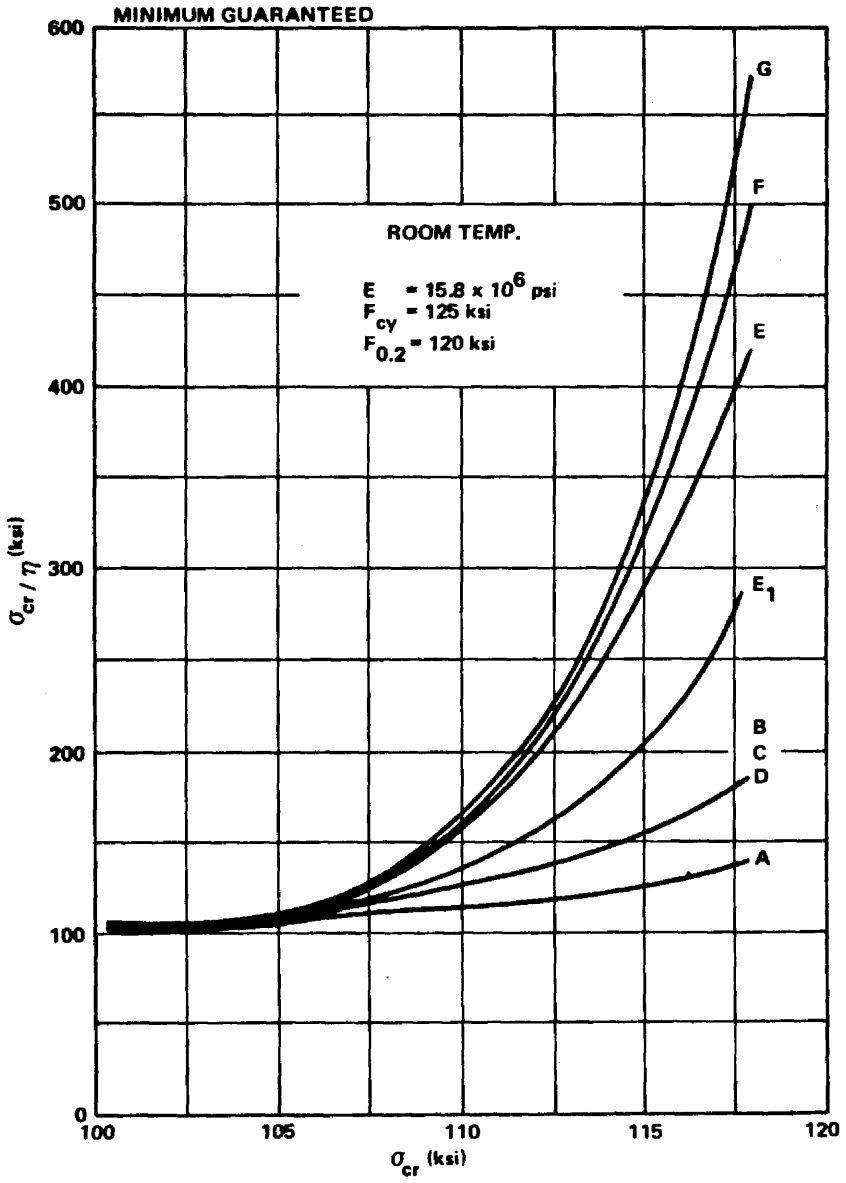

FIGURE 3.1-24. PLASTICITY CORRECTION CURVES FOR TITANIUM ALLOY SHEET < 0.25 6AL-4V ANNEALED LB0170-113

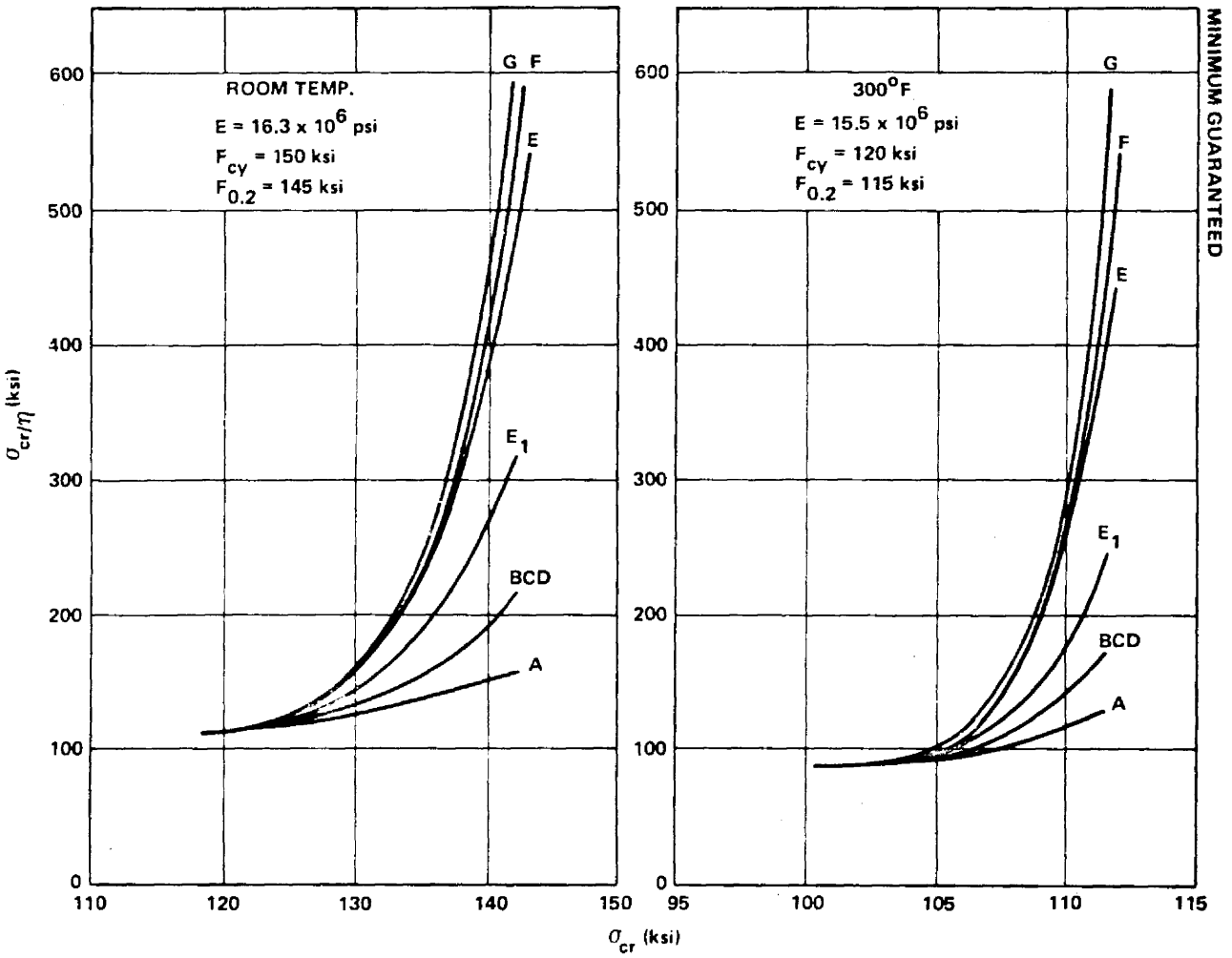

FIGURE 3.1-25. PLASTICITY CORRECTION CURVES FOR TITANIUM ALLOY SHEET < 0.25 6AL-4V CONDITION (SOLUTION-TREATED AND ANNEALED)

Although the value of μ is a function of the stresses for stresses in excess of the proportional limit, the plasticity curves were obtained assuming the conservative value of $\mu = 1/3$. The difference between using the value of $\mu = 1/3$ and $\mu = 1/2$ is small except for curves E and F.

It is worth noting that for curve A, $\eta = E_s/E$; for curve G, $\eta = E_t/E$ and, on the remaining curves, η is a function of both E_t and E_s. It can be seen that curves A and G bound the range of η. Curve G is the most conservative, whereas curve A results in the smallest possible reduction in the buckling load due to plasticity.